ATMOSPHERIC CONDENSATION

AND

MODELLING ITS NON-CONVECTIVE REGIME

BY

HILDING SUNDQVIST

DEPARTMENT OF METEOROLOGY
UNIVERSITY OF STOCKHOLM

LIST OF CONTENTS

INTRODUCTORY REMARKS

As dynamical models of the atmosphere have become more sophisticated and as the practical possibilities (such as computer capacity) are improving, the inclusion of condensation processes in the models gradually becomes more common and more elaborate. In modelling of the general circulation, it is of course a necessity to regard the release of latent heat as well as the formation and dissolving of clouds, because of their importance over longer time-spans, for the resulting motion (see e.g. Arakawa, 1975). But even in medium and short range forecasting, there is motivation for taking condensation into account. The more outstanding aims in that context are: inclusion of release of latent heat, prediction of precipitation and cloudiness, and calculations of the surface energy budget by taking a realistic cloud cover into account.

In the following lectures we will look into and discuss the atmospheric condensation processes. The intention is to eventually reach mathematical formulations that are suitable for incorporation in numerical weather prediction models. We shall begin with a review and a fairly superficial discussion of scales and effects of condensation with relation to the atmospheric motion. We will then proceed to a recapitulation of micro- and macro physical processes of condensation. Then a consideration of the formation of condensate, clouds and precipitation will follow. With the afore-mentioned survey as a background, we will then continue with a discussion of the formulation and inclusion of condensation in numerical prediction models. In that section we will dwell on parameterization problems and derivation of equations that describe non-convective condensation in a numerical model. Finally, a review will be given, however certainly not complete, of various approaches to including condensation in numerical prediction models.

In many of the discussions and reviews, detailed derivation and profound analyses will be left out (unless discussions arise during the lectures). We shall of course dwell upon those matters that may be considered to be of special relevance to the problem on formulating a set of equations that describes condensation in a numerical weather prediction model.

At the beginning of the chapters, there will be given a general reference to where a detailed and comprehensive analysis of the topic (alternatively, additional viewpoints) may be found.

As the disciplin of moist convective condensation will be covered in a separate series of lectures (R. Bates), those matters will not be taken up here except when it is felt necessary for consistency.

1 A REVIEW OF SCALES AND EFFECTS OF CONDENSATION IN THE ATMOSPHERE

General reference: Palmén and Newton (1969).

1.1 Scales and distribution of cloud systems

The scales of atmospheric condensation and accompanying clouds cover more or less the whole spectrum of sizes, from small cumuli to the vast cloud systems associated with the fronts of extra-tropical cyclones. There are, however, certain scales, that are more conspicous than others. The reason for this is that areas of condensation are closely related to atmospheric motion systems. The satellite pictures in Figures 1 and 2 give an idea of the typical cloud regimes that appear in the atmosphere. In Figure 1, we see for example the clouds associated with an extratropical cyclone and its front in the North Pacific, and the intertropical convergence zone (ITCZ) the clouds of which show up very clearly as a bright band near the equator over a substantial portion of the Pacific. In both the southern and northern hemisphere, we find small scale clouds which certainly are of the convective type, due to cold air outbreaks over warm water surfaces. Figure 2 exhibits cloud systems in the tropical regions. In the figure we can see the mesoscale regime, the cloud cluster regime, and the ITCZ. We may furthermore notice that the ITCZ, although being a persistant feature in the tropical regions, has a considerable day to day variation. We should also observe, for example in Figure 1, that the extratropical cloud systems, and the ITCZ system as well, typically have a width that rarely exceeds say 300-500 km. (For further examples of various cloud forms the reader

is referred to e.g. Andersson et al, 1966).

Condensation that appears on the smallest scales may, to some extent in some cases, be considered as solitary phenomena, e.g., a thunder cloud or a tornado. However, in most cases, the smallest scales are individual parts of a larger scale condensation regime, which is related to the synoptic scale situation. The fact that we have reasons to believe that this is so, is of fundamental importance with regard to our possibilities to describe condensation in numerical weather prediction models with the resolution that is commonly used. For example, the ITCZ and the so-called cloud clusters in the tropical belt are extensive ensambles of convective clouds. In middle and high latitudes, where we often observe cold air flowing over warm sea surfaces, we find fairly extensive areas of convective activity, the typical feature of which is probably governed by the large-scale flow and the potential instability of the air mass.

Let us look at the typical distribution of condensation and cloud systems in relation to weather motion with the aid of Figure 3. Besides getting an idea of the scales of the condensation systems, we also find the various types of condensation that appear. Hence we see the convection in the northerly flow in the rear of the cyclones, there are the nimbustratous-altostratous systems as a result of frontal upgliding, and in the warm sectors we find drizzle and fog as a result of isobaric cooling when the relatively warm air comes over colder water.

The topography of the earth's surface influences condensation and clouds in many different ways. For instance, on the windward side of a mountain slope we have a resamblance to the upgliding situation in frontal systems. On the lee side on the other hand, the air is often clear as a result of a downward motion. In certain situations, vertical oscillations are set up in the air that passes the mountain and a lee wave pattern is created, which sometimes may be observed to great distances downstream of the mountain. As another example, a coastal effect may be mentioned. When the wind is blowing parallel to the coast with the low pressure over the sea, a low level convergence zone near the coast

is created as a result of the stronger friction over land. This effect perhaps shows up more clearly in potentially unstable air, since the low level convergence then easily results in convective type condensation.

In the previous paragraphs, we have thus merely considered horizontal scales and spreading of condensation. It is also important to look at the vertical distribution. Cumulunimbi typically penetrate a great part of the tropospheric depth, whilst layers of stratus, stratocumulus or cirrus clouds usually are only a few hundred meters deep. The characteristic depth of nimubstratus clouds is fairly substantial. However, it seems to be a rule, rather than an exception, that this type of cloud contains strata of practically clear air. Figure 4 shows the cloud distribution, as deduced from observations from aircraft, relative to a warm front. The figure illustrates rather well what has just been said about vertical distribution.

1.2 Dynamical effects of condensation and clouds

The main dynamical effects of condensation are due to partly release of latent heat, partly the formation of clouds, which in turn influence the radiative processes.

The clouds influence the radiative processes in the atmosphere by reflecting short wave radiation and absorbing and emitting long wave radiation. These matters are of fundamental importance in long-range forecasting and climate modelling. An extensive analysis of these problems may be found in the report from the GARP/JOC Study Conference, 1974. In calculations of radiative processes, it is necessary to know not only the horizontal distribution of the clouds, but also the vertical, since the cooling rate at the top of the clouds is strongly dependent on their temperature. A quantitative illustration of this may be found in a paper by Manabe and Wetherald (1967).

The cloudiness situation affects, via the radiative processes, the energy budget of the earth's surface, which may be used for example in calculations of fluxes in the planetary boundary layer. In this respect, radiation calculations are of importance

in short and medium range forecasting as well, where a proper description of diurnal variations is of great interest.

The released latent heat by condensation acts as a direct thermodynamical heat source. Its importance for the evolution of the atmospheric motion systems depends on the type of condensation and its global location. For example, in a tropical cyclone the convectively released latent heat is the fundamental energy source for that system. The ITCZ is also vitally dependent on the heat provided by moist convection. The heat released by the convection in the trade wind areas and in the rear of frontal cyclones is probably of minor dynamical importance. This convection - and of course the more vigorous one mentioned earlier - constitutes, however, an efficient and important mechanism for turbulent fluxes of sensible and latent heat, moisture and momentum between the earth's surface and higher levels in the atmosphere.

Regarding the influence of the heat of condensation in extratropical disturbances, we may quote a concluding remark by Palmén and Newton (1969), "Without this additional heat source, polar front cyclones could not reach the intensities observed". We may realize the qualitative validity of this statement, by recalling that the release of latent heat in connection with frontal systems essentially takes place in the warm upgliding air. Energetically, this implies that the eddy available potential energy is increased. Furthermore, since the heating supports a direct circulation, that is, warm air is rising and cold air is sinking, the conversion from potential to kinetic energy is enhanced.

The frontogenetic influence of condensation has been treated in several papers. As examples, we may mention Eliassen (1959 and 1962) and Sawyer (1966). For illustration of that effect, Figure 5 shows two pictures from Sawyer's paper. In frame a), is depicted the transverse circulation in an assumed zone of confluence in a dry atmosphere. Frame b) shows the corresponding field of motion when condensation is permitted to occur. Comparing the two pictures we notice that the transverse circulation is intensified considerably in case b). We also notice that the ascending branch has a smaller horizontal scale in case b) than in case a).

Figure 6, from Danard (1964), depicts the vertical velocity calculated from real data using the ω-eq. Case a) is without and case b) is with inclusion of heating by condensation, which was deduced from the observed rate of precipitation. The results indicate that the heating causes a substantial strengthening of the vertical velocities, especially in the regions of ascending motion.

Several investigations of the effects of heating due to condensation have been made in numerical model experiments. Figure 7 illustrates an example of a clear - and improving - effect from inclusion of condensation heating in a 24 hour forecast. (After Bengtsson, 1967.) The results are from the SMHI three parameter filtered model with a grid distance of 150 km. In experiments with a primitive equation model, Lejenäs (1974) also reports similar results, that is, when the release of latent heat is taken into account an improvement in the forecast is observed as to the depth of a low pressure as well as to intensity and location of winds. In their GCM experiments, Manabe et al (1970) specially point out that the inclusion of heating from condensation results in a sharpening of the frontal zones and a more realistic magnitude of the mean zonal wind in the westerlies. Considering the results of this paper and the earlier one by Manabe et al (1965) and the results reported by Lejenäs (loc cit), we may infer that in order to achieve substantial changes (improvements) from the heating by condensation, it is necessary to have an adequate resolution in a model. This is consistant with what we have remarked upon in the previous, namely that the condensation tends to reduce the scales of, or to strengthen gradients in, the synoptic systems.

2 MICRO-PHYSICAL PROCESSES OF CONDENSATION

General reference: Mason (1971), Fletcher (1969)

When we begin the work on designing a condensation model for inclusion in a numerical prediction model, we will already at a fairly early stage find ourselves confronted with about the following sequence

of questions (at least if cloudiness is to be considered). How should the condensed water be distributed on clouds and precipitation; that is how do the cloud droplets that are suspended in the air grow to raindrops; what is, and which factors determine, the size distribution of droplets, is it dependent on the early stages of the condensation; hence what is the role of condensation nuclei and how does the phase transition from vapour to liquid come about? We shall now look into the enumerated questions - but in reversed order.

2.1 Condensation and condensation nuclei

Let us for the moment consider an atmosphere free from particles, but containing water vapour. Water molecules will by chance collide and occasionally form aggregates. These are unstable formations that re-evaporate unless a sufficient supersaturation exsists. Assuming a spherical form with radius r of the aggregate the following equilibrium relation may be derived.

$$(2.1) \quad E_r / E_\infty = \exp\left(2\sigma \frac{\varepsilon}{RTr}\right)$$

where E_r is the pressure of the supersaturated vapour, E_∞ is the saturation pressure at temperature T, over a plane water surface, σ is the so-called surface tension, R is the specific gas constant for air and $\varepsilon = 0.622$. We define supersaturation (or subsaturation) as

$$S = \frac{E}{E_\infty} - 1$$

where E is the current vapour pressure. If the supersaturation exceeds the critical value deduced from (2.1), then the aggregate will grow and act as a nucleus for further condensation. In a completely clean atmosphere, a supersaturation that amounts to 600-800 % is required for the so-called homogeneous nucleation to appear. Those values are never observed in the real atmosphere, because it contains particles of various kinds that act as conden-

sation nuclei. The required supersaturation therefore is less than 1 %, the exact value depending on, among other things, the size of the nucleus, its composition and surface structure.

The discipline of atmospheric nuclei is very vast in itself, but we shall confine ourselves to a few statements concerning this matter.

Let us first reconsider equation (2.1). When the condensation takes place on a hygroscopic particle, then the equilibrium relation is changed in such a way, that the right hand side of (2.1) should be multiplied with a quantity that is a function of the mass of the hygroscopic nucleus and the radius of the droplet. Furthermore, note that we now are considering very small supersaturations (10^{-2} and less), so we may approximate (2.1), by taking into account only the first term in a series expansion. Hence we obtain the following equilibrium relation

$$\frac{E_r}{E_\infty} = 1 + \frac{A}{r} - \frac{B}{r^3} \qquad (2.2)$$

where A is a function of the surface tension and temperature, and B essentially is a function of the mass of the hygroscopic substance. Thus the effect of a solution is to reduce the equilibrium vapour pressure for very small droplets; in fact, the condensation may start already around a relative humidity of 80 % on a sea salt nucleus. As the droplet grows and the solution becomes more dilute, this effect diminishes and the effect of the surface tension becomes dominating. Those features are illustrated in Figure 8. (Note the difference in scale above and below 100 %.) For example, a droplet of 0.1 μm radius and containing 10^{-15} g of salt in solution will continue to grow if the relative humidity is greater than about 87 %. If the cooling is strong enough to cause a supersaturation of about 0.12 % then we see that the droplet has reached a size of about 0.7 μm. This is the critical point for this particular droplet. It will now continue to grow - theoretically indefinitely. The further growth may, however, consume the vapour at a higher rate than the rate of production due to cooling. Consequently, the supersaturation will decrease and an immediate result of this is, that a re-evaporation begins of those

droplets that not yet have reached the critical point. This selection of activated condensation nuclei and also of the resulting droplet size distribution, is hence dependent on the type and size of nuclei that are present, and on the (large-scale) cooling rate of the air (Hindman et al, 1977).

The size and number of cloud droplets may hence be expected to be a function of the type of condensation nuclei involved, so let us look somewhat at the production and supply of those.

The major processes that produce condensation nuclei are

a) condensation and sublimation of combustion gases;
b) mechanical disruption of particles at the earth's surface;
c) collision between small (Aitken) nuclei with subsequent coagulation.

Process a) yields both insoluble and hygroscopic particles, of which many are very small. From b) we distinguish between nuclei of continental and maritime origin, the former being insoluable particles, while the latter are hygroscopic sea salt particles. The nuclei resulting from c) are of mixed chemical composition. The combustion and continental type nuclei are generally more abundant than those of maritime type. The latter are, on the other hand, the most efficient condensation nuclei. Thus, we may expect the number of droplets to be smaller and their size to be somewhat larger in clouds that are formed essentially on sea salt particles, than in clouds formed on continental type nuclei. This tendency is indicated by the diagrams in the Figures 9a and 9b.

2.2 Droplets; growth-rate, size distribution and concentration

The droplet growth by condensation hence takes place as a diffusion of water molecules from the vapour. At the same time, liberated latent heat is diffused to the ambient air. Considering these processes and assuming steady state conditions, we may derive the equation that describes the rate of growth of a droplet

$$(2.3) \quad r \frac{dr}{dt} = G\left(S - \frac{A}{r} + \frac{B}{r^3}\right)$$

where G contains the temperature, the thermal conductivity of the air and the diffusion coefficient of vapour. We shall only utilize (2.3) qualitatively. The two curvature terms on the right hand side can be neglected as the radius increases beyond the critical point. The rate of change of the radius is then proportional to the square root of time. A quantitative example of the growth rate is given in Table 1.

Table 1. Time of growth for a droplet by condensation.
Initial radius: 0.75 µm; supersaturation 0.05 %.

To radius (µm)	1	2	5	10	20	30
Time (s)	0.15	7.0	320	1800	7400	16000

There are two important features regarding the growth of droplets by condensation. The time required for a droplet to reach the zise of a drizzle drop (r = 100 µm) is unrealistically long. In that time, it is more likely that the droplet already has left the cloud and evaporated. The time it takes to reach a radius of 10-20 µm is fairly independent of the size of the nucleus that the condensation started on, because the smallest droplets will - as a result of their faster growth rate - catch up with the larger droplets. This implies, that the size distribution gradually becomes narrower as the condensation proceeds. In fact, the spectrum would be more sharply peaked than observed in real clouds.

We have already seen one example of droplet spectra (Figure 9b). In Figures 10a and 10b are shown mean distributions for various cloud types. In Figure 10a, with respect to droplet radius and in Figure 10b, with respect to liquid water content of the cloud. Both figures indicate that the clouds that are mainly non-precipitating have a relatively narrow distribution, while it is much wider for the clouds that typically precipitate. The characte-

ristics of non-precipitating clouds can essentially be explained by droplet growth by condensation (diffusion), while additional mechanisms must play an important role in featuring the broader spectra of precipitating clouds. Before discussing such mechanisms, let us first also get some idea of the concentration of droplets in clouds and their liquid water content.

In Table 2 we find, among other things, indications of droplet concentrations and liquid water content. We have already pointed out the difference between continental and maritime clouds. From the numbers given in Table 2, we may generally infer that non-precipitating and layer clouds have the higher concentration and the smaller droplet sizes. As to the liquid water content, there is a wide range of values and it is difficult to briefly summarize characteristics. We should also note that there is a pronounced vertical variation, which is examplified in Figure 11. This shows an average plot of airplane measurements in frontal cloud systems.

It seems that we may, in broad terms, say the following about the liquid water content. It varies between 0.1-4 g m^{-3} in convective clouds, the higher values applying to the middle and upper portions of cumulus congestus and cumulunimbus. In fog, the values lie between 0.1 and 0.2 g m^{-3} and for stratus and stratocumulus, a value of 0.3 g m^{-3} seems to be typical. For altocumulus, we may give the values 0.01 to 0.1 g m^{-3} with the lower values associated with lower temperatures. As guiding values for nimbustratus we may take 0.3-0.8 g m^{-3}.

Regarding mechanisms that can broaden the droplet spectrum, we should first mention the coalescence process, since it probably is the most important one. As the droplets are moving relative to each other - as a result of different fall velocities due to size differences, and of random motion - they may collide and possibly coalesce (fuse). The efficiency, with which this accretion process can take place, depends on the ratio of the radii between the larger (collector) and the smaller droplets. Once the collector has grown somewhat, then it is essentially the difference in fall velocity that gives a motion relative to the smaller

Table 2. Characteristics of cloud-droplet populations (after Mason, 1971).

r_{50} the median radius; half the droplets have radii smaller (or larger) than this value;
r_d the mode or most frequent radius, i.e. the radius corresponding to the peak of the curve;
r_m the mean radius, i.e. the sum of all the droplet radii divided by the total number of droplets.

Cloud type		Author	r_{min} (/um)	r_{50} (/um)	r_d (/um)	r_m (/um)	r_{max} (/um)	$n(cm^{-3})$	$w(g\ m^{-3})$
Small continental cumulus									
(7000 ft)	Australia	Squires	2.5	6	-	-	10	420	0.4
	U.S.A.	Weickmann & aufm Kampe	3		6	9	33	300	1.0
	England	Durbin			4	6	30	210	0.45
	Russia	Kazas			4.3	4.7		310	0.15
	U.S.A.	Draginis		6	7			300	0.40
Small maritime cumulus									
	Hawaii	Squires	2.5	12	11	15	20	75	0.50
	Caribbean	Draginis		9	11			45	0.4
Cumulus congestus									
	U.S.A.	Weickmann & aufm Kampe	3		6	24	83	64	2.0
(600 m above base)									
	Russia	Zaltsev	2		5.5		40	95	0.45
Cumulonimbus									
	U.S.A.	Weickmann & aufm Kampe	2		5	20	100	72	2.5
Altostratus									
	Germany	Diem	1		4.5	5	13	450	
	Russia	Kazas			4.6	6.6		220	0.6
Nimbostratus									
	Germany	Diem	1		4	6	20	330	
Stratus									
	Germany	Diem	1		4	6	22	260	
	Hawaii	Squires	2.5	13			45	24	0.35
Stratocumulus									
	Germany	Diem	1		3.5	4	12	350	
	England	Frith	3				25	500	
Orographic cloud									
	Hawaii	Squires	5	13			34	45	0.30

droplets. We may then derive the following equation, describing the rate of change of the collector radius

$$(2.4)\quad \frac{dr}{dt} = \frac{E'}{4\rho_L} w (V - v)$$

where E' is proportional to the collection efficiency, w is the liquid water content, V and v are the fall velocities of the collector and smaller droplets respectively, and ρ_L is the density of water. The vertical velocities may be described according to Stoke's law, that is, proportional to r^2, for radii smaller than about 50 μm. For larger droplets or drops, the fall velocity is approximately proportional to r or $r^{1/2}$. The collection efficiency will approach unity as the droplet grows. Thus, the increase of the collecting droplet will take place at an accelerated rate, provided the liquid water content is maintained. We will come back to eq. (2.4) in connection with the precipitation process.

It appears to be a common opinion that the radius of the collecting droplet at least has to be 19 μm before the coalescence process can begin. Since it in some cases seems unrealistic that the droplet growth by condensation could produce droplets as large as 19 μm - yet these sizes are observed - then an explanation other than coalescence or straight condensation has to be found. It has been suggested that turbulent motion and random fluctuations in the supersaturation could allow a sufficient number of droplets to grow to those sizes that are necessary for the coalescence. In a study of this nature, Mason and Jonas (1974) found, that among the parameters introduced, the environmental lapse rate and humidity were quite influential.

Our next step in this survey is now to follow the further evolution of the droplets until they reach raindrop size. A growth to considerable sizes is namely necessary, because when the raindrop leaves the cloudbase, it will be subject to evaporation in the unsaturated air below the cloud. We may realize this by utilizing eq. (2.3) with a given negative supersaturation, say $S = -0.2$. A droplet with an initial radius of 10 μm has evaporated after a falling distance of 2 cm; for the initial radii of 30, 100, and

150 µm, the corresponding distances are 1.7 m, 208 m and 1 km.

2.3 Release of precipitation

In considering processes resulting in the release of precipitation, it is material to first recapitulate some of the characteristics of freezing and sublimation in the atmosphere. The situation regarding spontaneous, or homogeneous, freezing is quite similar to the one of homogeneous condensation. Here instead, a pronounced supercooling (down to -35 to -40°C) is required. However, particles of various types may act as freezing nuclei. Particles, originating from the earth's surface and having the right structure, may initiate freezing already around -15°C. Ice crystals, that are already formed, as well as debris from crystals that have broken up, are able to cause freezing at levels of a temperature -10 to -15°C. Ice particles introduced amongst supercold droplets in that temperature interval normally become subject to a fast growth. The reason for this is that, at a given temperature, the equilibrium vapour pressure over ice is lower than over water, why an evaporation with an accompanying sublimation occurs. Let us also note that some artificially produced freezing nuclei are even more efficient than ice particles.

Thus, only some of observed cirrus clouds may possibly have resulted from homogeneous freezing, but the majority of clouds consisting of ice are formed from supercooled droplets whose freezing is facilitated by the presence of various freezing nuclei.

It was these considerations that formed the foundation of the suggestions by Wegener (1911) and Bergeron (1935) regarding the release of precipitation in clouds. As the ice particles gradually acquire more mass, they start to fall and as they reach the melting level, some of them might stick together after collision and hence quickly form even larger elements. These may then efficiently collect smaller droplets during the continued fall through the cloud.

The equation that may be derived for the rate of growth of an ice crystal due to the evaporation - sublimation process is similar

to eq. (2.3), without the curvature terms, and the supersaturation is then taken with respect to ice. An equation, symbolically similar to (2.4), may also be derived for the accretion-aggregation process. Dealing with ice, the rate of change of mass is considered instead of radius, which is more commonly used in the liquid phase.

For a long period after the appearance of Bergeron's paper, it was considered that his proposed mechamism was the only one for initiation of precipitation. It is probably the most important mechanism in extratropical regions, but it cannot provide a reasonable explanation in all cases. The following qualitative statement by Mason (1971) is quite persuasive: "However it must have been obvious to both meteorologists and aviators that in tropical regions showers often fell from clouds whose tops did not reach within thousands of feet of the $0^{o}C$ level." Specific observations in tropical regions do show that heavy rain falls from clouds that are warmer than $0^{o}C$.

As the increase of mass takes place at an accelerated rate both in the accretion-aggregation and coalescence processes, both these are capable of producing sufficiently large elements for precipitation to occur in reasonable time. Factors - except for those included in eq. (2.4) or its analogue in the ice phase - that are decisive for the size of the rain drops when these leave the cloud are the thickness of the cloud, the vertical velocity of the air, and possible turbulent motion in the cloud. A droplet is carried upwards as long as its fall velocity is smaller than the upwind of the air, but the increase of mass eventually results in a fall velocity that is larger and the drop starts to descend relative to the earth's surface - the drop precipitates. The droplet/drop will gain mass both on its way up and down. Since the length of the path is a function of the upwind of the air, the importance of the latter is obvious. If the motion is turbulent in the cloud, a precipitating drop might be caught by the stronger winds and carried upwards again, thus acquiring additional mass before leaving the cloud. The thickness of the cloud is an important parameter as well. If the cloud is too shallow, the droplet will pass through the top of the cloud and evaporate, before the mass has become large enough to cause a downward motion. Furthermore,

we may note that a droplet formed at a higher level will result in larger raindrops leaving the cloud base than droplets formed at lower levels, because the former will have a longer descending path through the cloud than the latter. An implication of this is also that the size spectrum of raindrops tends to widen as the thickness of the cloud increases.

2.4 Some comments on the macro-scale phase

In the foregoing subsections, a couple of remarks have been made in passing, regarding large-scale aspects. (Here "large-scale" is used for denoting lateral scales from cumulus size and larger, and vertical dimensions from say 100 m and bigger.) We shall here merly summarize some matters regarding relations between micro- and macro-scales. Some of the questions will be discussed further, when we are concerned with the subject of parameterization in the next chapter.

The most dominating large-scale parameters are of course vertical velocity, temperature, lapse rate and humidity. But we should also mention the shape of the earth's surface (orography) and the aerosol situation. The latter influences the size distribution and concentration of cloud-droplets, which in turn govern the radiative properties of clouds (see e.g. Fitzgerald, 1974, and Twomey, 1976).

The vertical velocity very much determines the liquid water content of clouds, and (jointly with lapse rate and humidity) it also governs the replenishment of water. Both the liquid water content and the rate of precipitation increase with an increasing vertical velocity (e.g. compare convective with layer clouds). The temperature also controls the liquid water content, since the maximum amount of vapour in the atmosphere is a function of temperature. Ice crystal production is of course strongly dependent on temperature. The altitude of a cloud, or its thickness, could alternatively be regarded as the important parameters as to the number concentration of ice crystals.

Temperature is the decisive parameter for the form - rain or snow - in which the precipitation reaches the ground. Such a distinction is dynamically significant, especially in models of the general circulation and of the climate, because of its impact on the radiation conditions at the earth's surface.

A basic condition for snow to appear is, of course, that some part of the cloud has a sufficiently low temperature for ice crystals to be created. The altitude of the $0^{\circ}C$ isotherm and the lapse rate then determines whether the crystals/snowflakes will melt or not. Using the typical fall velocity of about 1 m/s for snowflakes and a precipitation rate of 1 mm/h and utilizing expression (3.15)(Section 3.1.1), we find that the melting process is completed after a falling distance of about 300 m from the freezing level if the lapse rate is $6.5^{\circ}C/km$

Orographic effects on rain fall may be substantial. This is documented in several observational studies (see e.g. Bergeron, 1965). The orographically induced cloud may, in itself, be too shallow to permit an efficient coalescence and rainfall. Bergeron suggested that the precipitation from a higher level cloud, produced by the synoptic situation, may bring about an effective wash-out, thus resulting in a heavy rainfall. Quantative results from model studies (Storebø, 1976, Bader and Roach, 1977) support this hypothesis. From our point of view, it is also pertinent to note that the scale of this enhanced precipitation-rate is closely related to the orographic scale.

The influence of the thickness of a cloud is illustrated in Figure 12. It is a rough composite of reports from observations (see Mason's book pp 289-290). Thus, clouds having a thickness less than about 500 m very seldom produce any precipitation and in order to evolve continuous precipitation, the cloud has to be about 2.5 km thick.

Regarding time scales, it appears that a turnover time of the cloud water content is a suitable measure for our purpose. The typical scale may then be considered to reflect an average time, required for cloud droplets to be converted to raindrops

in precipitating clouds, or a mean residence time of the droplets in non-precipitating clouds. From results of theoretical studies and observations (see Mason, 1971) we find that the typical time scale for precipitating layer clouds is of the order some hours, and for shower clouds around tens of minutes.

Raindrop-size spectra have been investigated observationally, and consequently suggestions of various mathematical descriptions of the distributions have been made (see Mason, 1971). The most commonly used function is due to Marshall and Palmer (1948) and it has the following form

$$N = N_0 \, e^{-\lambda D} \tag{2.5}$$

where D is the drop diameter and N_0 and λ are empirical parameters. Relation (2.5) expresses the number of drops per unit volume per unit diamter length; that is, $N \cdot \Delta D$ expresses the number-concentration of drops in the interval D to $D + \Delta D$. To exemplify the use of this relation, we calculate the concentration of rainwater

$$M_R = \int_0^\infty \frac{4}{3} \pi r^3 \rho_L N \, dD = \tag{2.6}$$

$$= \frac{\pi \rho_L}{6} \frac{N_0}{\lambda^4} \int_0^\infty (\lambda D)^3 e^{-\lambda D} \, d(\lambda D) =$$

$$= \pi \rho_L N_0 \lambda^{-4}$$

With the aid of (2.5), we may also calculate an average fall velocity of the rain, which combined with (2.6) gives the rate of precipitation. This relation may then be used for determination of N_0 and λ from observational data.

Let us finally also state that the typical rainfall rates are about a few mm/h, and a couple of tens of mm/h from layer clouds and shower clouds respectively.

3 ON INCLUSION OF CONDENSATION IN NUMERICAL PREDICTION MODELS

General reference: Kessler (1969), Ogura and Takahashi (1971).

In these lectures we shall make an attempt to analyse the problems (at least some) that are connected with the description of condensation in numerical prediction models; that is, variables are available at a resolution of 100 km or coarser in the horizontal, and 1-3 km in the vertical. In order to be able to carry out numerical integrations in reasonable time, we thus have to investigate the possibilities to paramterize.

The first part of the discussion is intended to lead us to a principal formulation of a condensation model in this context. In the second part, we will then derive a fairly simple specific model that treats not only the release of latent heat and precipitation, but also the liquid water content of clouds. Some quantative results of this model will also be presented.

Before proceeding to the actual discussion, let us again remark that we are here considering non-convective type of condensation. At the same time, it seems natural to make a comment on the use of the terms "small-scale" and "large-scale" in this context. They are often meant to distinguish between convective and non-convective type of condensation. However, in numerical modelling, those terms are more suited for reference to the resolution. With the resolutions that we are having in mind, both convective and non-convective type of condensation may very well be small-scale - or "subgrid scale" that we should rather use. The term "large-scale" will be used as denotation of scales that are resolvable by the grid applied to the model.

Unless specially remarked, numerical values are given in SI-units.

3.1 Parameterization of non-convective condensation; principle formulation of model equations

In order to recall the concept of parameterization, let us for the moment assume that we have derived a complete set of equations

that describe the atmospheric motion, including the micro-physical evolution of the condensation processes. Then, when we have settled what resolution we will (or are able to) use in the numerical treatment, we will find that some of the prognostic equations and dependent variables demand a higher resolution. Thus, some of the equations have to be abandoned, yet at least some of the unresolvable dependent variables have to be retained in the remaining system (if we persist in taking condensation into account). The obvious consequence of this is that we have got more dependent variables than we have equations - the system is no longer closed. In order to obtain closure conditions, we then search for relations between the average (statistical) effects of the subgrid scale actions and the resolvable (large-scale) variables of the system. Those relations hence constitute the parameterization of subgrid scale condensation processes.

The formulation of such relations cannot, in all cases, be entirely based on stringent physical reasoning, but we have to resort to plausible hypotheses, because we are lacking knowledge of the details of the processes that we try to describe. The derived formulations have to be tested from various points of view. For example, sensitivity, range of validity (e.g. we have to employ different formulations for convective and non-convective situations), and numerical values of constants and parameters that have been introduced.

We have already noted that the clouds or condensation regions that we find important to consider are not necessarily fully resolvable by the model grid. Consequently, we have to parameterize not only the micro-physical processes, but also the evolution of cloud and precipitation areas. It will be advantageous to divide our discussion into two major parts; in the first one we will treat the parameterization of the micro-physical processes, and in the second one, we shall consider the special problems that are connected with the fact that the clouds, at least in some cases, must be treated as subgrid scale entites.

3.1.1 Parameterization of micro-physical processes

To make the discussion as straight as possible, we will first establish the formal set of equations that is relevant to our problem. The various terms will then be discussed separately. We will utilize a paper by Ogura and Takahashi (1971) in those parts that are not specific to convection.

The momentum equations will be omitted and we will consider the thermodynamic equation and the rate of change (continuity) equations for the various forms that water appears in, and the p-system is adopted. The source and sink terms that we shall take into account are:

S1 rate of condensation;
S2 rate of conversion of droplets to drops;
S3 rate of production of ice crystals by freezing of raindrops;
S4 rate of sublimation of vapour to ice crystals;
S5 rate of melting of ice crystals;
S6 rate of evaporation of droplets;
S7 rate of evaporation of drops;
S8 rate of evaporation of ice crystals.

Other terms will be included symbolically with the aid of the operator $A(\quad)$, in which the dynamical terms are the primary ones. Hence,

$$A(\ ) = -\nabla\cdot[v(\ )] - \frac{\partial}{\partial p}[\omega(\ )]$$

Our set of equations then is:

$$(3.1)\quad \frac{\partial\theta}{\partial t} = A(\theta) + \frac{\theta}{T c_p}\left[L_v S1 + L_s S4 - L_v S6 - L_v S7 - L_s S8 + L_f (S3 - S5)\right]$$

$$(3.2)\quad \frac{\partial q}{\partial t} = A(q) - (S1 + S4) + (S_6 + S7 + S8)$$

$$(3.3)\quad \frac{\partial m_c}{\partial t} = A(m_c) + S1 - S2 - S6 - \frac{\partial}{\partial p}(\omega_c m_c)$$

$$(3.4)\quad \frac{\partial m_r}{\partial t} = A(m_r) + S2 - S3 + S5 - S7 - \frac{\partial}{\partial p}(\omega_r m_r)$$

$$(3.5)\quad \frac{\partial m_i}{\partial t} = A(m_i) + S3 + S4 - S5 - S8 - \frac{\partial}{\partial p}(\omega_i m_i)$$

where q is the vapour mixing ratio, m is the condensate mixing ratio and the subscripts c, r and i denote droplets, drops and ice-crystals respectively, the subscripted omega is the fall velocity ($\omega_{c,r,i} > 0$) of respective category of condensate. L_v, L_s and L_f are the latent heat of respectively evaporation, sublimation and fusion. Quantities not mentioned have their conventional meaning.

The rate of precipitation is defined as the downward flux of mass of water (usually measured in mm/h) through a horizontal surface - or in our case through a surface of constant p. As m_r and m_i constitute the precipitating substance of the above system, we obtain the rate of precipitation at a level p, $\tilde{P}(p)$, as

$$(3.6)\quad \tilde{P}(p) = \frac{1}{g}\left[(\omega + \omega_r) m_r + (\omega + \omega_i) m_i\right]_{p=p}$$

For reference later on, we shall establish the formal relation between the rate of precipitation and the above equations. This is obtained by summing (3.4) and (3.5) and then integrating from the top of the cloud (where , by definition, the mass of liquid and solid water is zero) and a level p. Hence

$$(3.7)\quad \tilde{P}(p) = \widetilde{S2+S4} - \widetilde{(S7+S8)} - \frac{\partial}{\partial t}\widetilde{(m_r+m_i)} - \nabla\cdot\widetilde{\left[V(m_r+m_i)\right]}$$

where

$$(3.8)\quad \tilde{(\ )} = \frac{1}{g}\int_{P_{top}}^{P} (\ )\, dp$$

Now considering our closed system of equations (3.1)-(3.5), we find that there are no explicit tendency equations for those processes or mechanisms that the terms S1-S8 stand for. Those must therefore be expressed in terms of the quantities that we have available; in short, we have to parameterize. This also applies to the fall velocities, which strictly should be averages with respect to the size spectrum of respective type of condensate. We shall now describe the parameterizations in more detail.

S1 The required supersaturation is practically always less than 1 %, so we may assume that the condensation occurs when the relative humidity is 100 %. If we consider the equations that describe the growth of a population of droplets, we will find that, assuming that the relative humidity (supersaturation) is in a quasi-steady state, the rate of formation of droplets - i.e. condensation rate - is proportional to the convergence of water vapour (Mason, 1971, pp 125-127). Hence, in our case, we will obtain the rate of condensation from the rate of change of q. The practical procedure will be indicated later on.

S2 This term should describe the various phases of the coalescence process, implying that the spectra of droplets and drops ought to be taken into account. Let us nevertheless make a simplified analysis by regarding merely the coalescence equation (2.4). We rewrite this equation in terms of the mass of the collector, m_r. Neglecting the fall velocity of the droplets and since V is proportional to some power of the collector's radius we get

$$(3.9)\quad \frac{dm_r}{dt} = \rho_L^{-1} E'' m_c \left(\rho_a m_r\right)^{1-b/3}$$

where E'' is essentially a function of the collection efficiency. The value of the parameter b depends on the fall velocity. For drop radii smaller than 50 µm, b = -1 and for radii larger than about $\frac{1}{2}$ mm, b = 0.5. A good approximation for intermediate sizes appears to be b = 0. The proportionality constant that is connected with the fall velocity, and now contained in E'', has widely different values for the three values of b. We shall further discuss this approach later on. For the moment we shall instead briefly study Kessler's (1969) proposals. He splits this process up into two parts, one called auto-conversion and the other collection. The former is connected to the coalescence that appears as a result of relative motion between cloud droplets. Collection considers the coalescence that results when a raindrop sweaps through the cloud. Since non-precipitating clouds have a relatively low water content, Kessler proposes that this has to reach a certain threshold value, a , before the auto-conversion comes into action. It is then assumed to be a linear function of the mass of water contained by droplets. Hence

$$(3.10)\quad \left(\frac{dm_r}{dt}\right)_{auto\text{-}conv} = k_1 (m_c - a)$$

The numerical values of k_1 and a are most likely functions of the large-scale vertical motion, such that they show a tendency to decrease for decreasing magnitude of the vertical velocity.

The collection is treated more rigiorously. Here Kessler starts from the coalescence equation for an individual drop and then integrates over all particles, taking a proper weighting of size distribution into account. The Marshall-Palmer distribution was used. Then in our notations

$$(3.11)\quad \left(\frac{dm_r}{dt}\right)_{collect} = 3 \cdot 10^{-1} N_0^{1/8} m_c m_r^{7/8}$$

in which the collection efficiency has been taken to unity and included in the numerical constant. The interesting thing to note here is that the distribution parameter N_0 - which in itself has proven to be practically constant over a wide range of

rainfall rates - appears to the power 1/8, implying that the expression is insensitive to possible uncertanties in this parameter. Note also, that this mechanism does not start to function until raindrops exist. Thus, we finally obtain

$$(3.12) \quad S2 = k_1 (m_c - a) + k_2 m_c m_r^{7/8}$$

$$k_2 = 2.2 \quad s^{-1}$$

We may also note, that Ogura and Takahashi assumed S2 to be directly proportional to the cloud water content.

S3 Since we have not derived a separate equation for small ice particles that would be part of the cloud structure, we postulate that only raindrops may freeze. A reasonable description of such a glaciation process is then to assume that the rate of production is proportional to the raindrop mixing ratio:

$$(3.13) \quad S3 = k_3 m_r$$

Ogura and Takahashi allowed this process to take place as soon as the temperature was below 273K, and the proportionality factor was independent of height (or temperature). As mentioned earlier, data from laboratory work and from observations of real clouds evidence that the probability for glaciation of drops is a pronounced function of temperature. A plausible approach would thus be to have $k_3 = 0$ for $T > 269$K, and the maximum value should not be reached until, say, $T < 248$K. It appears difficult to assess proper values for k_3, without guidance from numerical experimentation.

S4 Here, we do not go into details of how the sublimation starts, but just assume that the ice particles increase according to the diffusion equation applicable for ice (see e.g. Mason, 1971, p 277). We furthermore assume that the ice particles are distributed according to the Marshall-Palmer distribution and then we integrate in the same way as described for S2, obtaining

$$(3.14)\quad S4 = k_4\, \rho_a^{-1/2}\, S_i\, m_i^{1/2}$$

$$k_4 \rho_a^{-1/2} \simeq \begin{cases} 4\cdot 10^{-5} & T \simeq 265\,K \\ 0.5\cdot 10^{-5} & T \simeq 250\,K \end{cases}$$

where ρ_a is the air density and S_i is the supersaturation with respect to ice, that is, in the definition of S in Section 2, we replace the vapour pressure in the denominator by the vapour pressure with respect to an ice surface. The parameter k_4 is slightly temperature dependent, because the saturation vapour pressure is involved. The two values given above appear to be reasonable. A very important aspect to keep in mind is that the sublimation process does not become pronounced, unless the temperature is lower than about 260K. A conceivable way of accounting for this effect would be to multiply k_4 by a factor that has a very small value for temperatures higher than 265K and that then increases for decreasing temperature until unity is reached around 245K.

S5 Here we follow a reasoning that is analogous to the one for S4, but instead we now have to consider the excess temperature above 273K (Mason, 1956). Utilizing numerical values indicated by Ogura and Takahashi, but disregarding the ventilation effect, we obtain

$$(3.15)\quad S5 = 10^{-4}(T - 273)\, m_i^{1/2}$$

S6 Regarding these processes, we could of course utilize the diffusion equations for droplets and ice crystals. For instance, for the latter, we would then use the expression for S4 with a reversed sign and the proper subsaturation included (note from equations (3.1, 3.5) that we have defined S1-S8 as positive quantities). However, we have already observed that the evaporation proceeds very

fast for small droplets, and ice crystals as well, so it appears satisfactory to just assume that those evaporate immediately, when they are subject to subsaturation. This is also verified by numerical experiments that Ogura and Takahashi made.

S7 and S8

In order to express the evaporation from raindrops, we utilize an approximate version of the diffusion equation due to Kessler. In deriving this, he disregards the necessary diffusion of heat towards the drops and merely considers the diffusion of vapour away from them. Then, adopting the Marshall-Palmer distribution, he obtains

$$S7 = 6 \cdot 10^{-2} q_s S (\rho_a m_r)^{13/20} \tag{3.16}$$

where q_s is the saturation mixing ratio of vapour.

Fall velocities As mentioned earlier, we have to deduce a representative value for the fall velocity of the hydrometeors. Formulas for the fall velocities may be found for example in Mason (1971). To obtain reasonable values for the drops and the ice crystals respectively, we apply the Marshall-Palmer distribution and as an example, we give the resulting expression for the average fall velocity of raindrops, according to Kessler

$$V_r = 12 (\rho_a m_r)^{1/8} \tag{3.17}$$

In our system, we have to transform to a p-velocity with the aid of the hydrostatic equation. A formally similar equation for the ice crystals may be obtained. Reference is here made to Ogura and Takahashi, who derive the formulas in a somewhat different way from what Kessler does. Note, that the terminal velocity is fairly insensitive to fluctuations in the mass of precipitating substance, because of the very small exponent in the expression.

Concerning cloud droplets, it is often considered that those share the motion of the air, thus having zero fall velocity. This

assumption are made in connection with modelling of convective clouds, where it is certainly legitimate with regard to the large vertical velocities of the air. In non-convective type of condensation this approximation may be questionable since the vertical velocity then is typically no larger than of the order of 10 cm/s, which approximately is the terminal velocity for a 30 /um droplet.

If we consider the fall velocity of a droplet

$$(3.18) \quad v_c = 1.2 \cdot 10^8 \, r^2$$

and the log-normal distribution, which often is adopted for droplets (see Matveev, 1967, for details)

$$(3.19) \quad f(r) = (r\sigma\sqrt{2\pi})^{-1} \exp\left[-\frac{(\ln r - \ln r_0)^2}{2\sigma^2}\right]$$

$$\ln r_0 = \overline{\ln r} \Rightarrow r_0 = \sqrt[n]{r_1 r_2 \ldots r_n}$$

$$\sigma^2 = \overline{(\ln r - \ln r_0)^2}$$

we may get an estimate of their representative fall velocity from

$$(3.20) \quad \overline{v_c} = \int_0^\infty v_c f(r)\, dr = 1.2 \cdot 10^8 \, r_0^2 \, e^{2\sigma^2}$$

Taking the values $r_0 = 7$ /um and $\sigma = 0.58$ (corresponding to an arithmetic mean radius of about 10 /um) from Matveev's book, we get a value of 1.2 cm per second.

In order to get an idea of the principal practical procedure, we will follow a sequence of events as they will appear when condensation starts in the above model. Hence, we presume a prevailing convergence of water vapour as a result of the large-scale motion, tending to yield a moisture content in excess

of the saturation value. At the moment just prior to the onset of condensation, there is no liquid or solid water present, implying that none of the mechanisms S2-S8 will be involved. All excess vapour will go into S1, so that the current vapour mixing ratio will be kept at saturation. From (3.3) we see that cloud droplets now will be created by S1. As long as the mixing ratio of cloud droplets is less than a (see 3.12), the only operating mechanisms will be S1 and S6, because all the others require the existence of raindrops or ice crystals. At the moment when the threshold a is passed, then S2 will be non-zero and consequently raindrops will appear, as seen from eq. (3.4). Now S3 (3.13) will start at appropriate temperatures and at the next moment ice crystals will be created, according to eq. (3.5). With the prescence of ice crystals, the mechanism S4 (3.14) also will be operating, as well as the evaporation and melting processes. From now on, all the cogs of the machinery are engaged and jointly contribute the cloud structure and precipitation.

As we realize from the above paragraph, the influences from some of the mechanisms will lag by one time step in some of the prognostic equations. This is probably not severe from an accuracy point of view, provided that the time step is short relative to the characteristic time scales involved. The degree of accuracy is somewhat dependent on the precise numerical formulation, on which we will not dwell here. However, there seems to be a pitfall, regarding energy consistency, that warrants some comments. For simplicity, we shall regard the moment when condensation commences. Then, since q exactly should be at saturation, we may express it in terms of temperature, implying that we may rewrite the left hand side of (3.2) as a factor, for the moment called F, times the time-derivative of θ. By combining (3.1) and (3.2), we then eliminate the time-derivative, and we obtain a diagnostic equation for S1 of the following symbolic form (a more detailed derivation will be carried out in section 3.2)

$$(3.21) \qquad S1 = (1+F)^{-1}\left[A(q) - F\frac{c_p}{L_v}\frac{T}{\theta}A(\theta)\right]$$

where F is a positive quantity directly proportional to the saturation mixing ratio. Taking standard atmosphere values, F is about 0.25, 1 and 2 at the pressure levels 400, 700 and 1000 mb respectively. The very important observation to be made is that not all of the apparent excess humidity, resulting from large-scale convergence, can be used for condensation. The reason for this is that the condensation is a wet-bulb type process. That is, when some vapour condenses, the temperature rises and consequently some vapour has to be used for keeping the humidity at the saturation value. This is why F appears in the denominator of (3.17). When all the mechanisms are at work, we cannot strictly derive such a simple diagnostic relation, but it is probably accurate enough to utilize the values of the processes of the previous time step. We may, for example, specially note that the right hand side of (3.17) will be reduced due to the existence of S4, which presumes that some of the vapour is utilized for sublimation.

Since we are dealing with layer clouds, it may also be important to pay attention to their thickness. In Subsection 2, we noted the empirically found qualitative correlation between the cloud thickness and precipitation (Figure 12). A conceivable approach towards more realistic situations would thus be to introduce a threshold thickness in the second term of eq. (3.12) and to let k_2 be an increasing function with thickness, from $k_2 = 0$ at the threshold to $k_2 = 2.2$ for thicknesses greater than 2.5-3 km. Measures of this kind naturally presuppose an adequate vertical grid resolution. With regard to the definition of the auto-conversion process, it seems reasonable to assume that this is fairly independent of the cloud thickness.

We could readily imagine several ways of extending the above model by taking additional details into account. An approach of this type is justified in specific studies of the cloud dynamics, which provide insights that are material for deducing parameterization schemes. We will nevertheless take a step in the opposite direction, i.e. to consider lumping some of the details together, because the above model is probably already too complex and time-consuming in connection with practical numerical weather prediction. So let us briefly analyse the implications of such an approach,

by stepwise omitting the details of the above model system.

As the first step, assume that we abandon the possibility to distinguish between water and ice in the precipitating substance. Then, we can no longer discern the conversion between drops and crystals (S3 and S5), which also is evident from the sum of equations (3.4) and (3.5), which now becomes the appropriate equation for the precipitating hydrometeors. Hence

$$(3.22)\quad \frac{\partial m_{Hi}}{\partial t} = A(m_{Hi}) + (S2+S4) - (S7+S8) - \frac{\partial}{\partial p}(\omega_{Hi} m_{Hi})$$

where the meaning of the indices is obvious. Furthermore, S7 and S8 merge into one joint process. Regarding S4, this also disappears, which implies that all the condensation is taken up by S1, as realized from equations (3.1) and (3.2). The conversion of droplets to drops is then indirectly affected, according to equation (3.3).

Now, we could conceive of employing this simplified model under the assumption that all condensate appears in liquid form. This would probably not be a too severe approximation as to the amount of heat released by the condensation. However, we have earlier noted, that ice crystals have a substantial impact on the release of precipitation. A plausible way of accounting for this would be to introduce parameters in S1 and S2, so that the principle features of the formation of ice crystals would be reflected. Such parameters implicitly imagine some ratio between crystals and drops. This ratio should then be applied in the calculation of a representative fall velocity. For strict consistency, those parameters should be properly regarded even in S6.

A next natural step to further simplification of our cloud model is to give up the explicit calculations of the precipitating water and to merely retain the cloud water equation. As a consequence of this, we have to reconsider the mechanisms S2 and S7, because their present forms are functions of the precipitation mixing ratio. By this second step of approximation, we are loosing insight into the detailed substructure of the total water

amount, released by condensation. In order to enable calculation of how the total water is sub-divided on cloud and precipitation, it is still necessary to know the conversion rate of droplets to drops (S2), as seen from equation (3.3). This conversion, now has to be related to the cloud water mixing ratio. A specific formulation of S2 will be discussed in Section 3.2 We may note, that the rate of precipitation is still obtainable despite the missing precipitation content. Instead of (3.6), we now use (3.7), which reduces to a diagnostic equation, since the two last terms have to be neglected.

It is pertinent to make an observation that applies to both of these simplified versions. Namely, the same source and sink terms now appear in both equation (3.1) and equation (3.2). We may therefore join those terms into one, and then work with the net condensation rate.

Let us also mention the further simplification that implies that we leave out calculations of cloud water content. Besides the release of latent heat, we are then merely able to calculate the rate of precipitation, by assuming an immediate fallout of the condensate. This has been the usual approach in calculations of non-convective condensation in numerical weather prediction models. An additional remark is pertinent. Namely, this assumption implicitly assumes a steady state in the relative humidity and a value less than 100 % is often adopted. Then note - since the release of latent heat, by and large, is proportional to the vapour convergence - that the heating rate is accordingly smaller than if the true saturation value were used. Alternatively it may be regarded as a consequence of limiting the maximum possible vapour content of the atmosphere to a value smaller than the saturation value.

3.1.2 Parameterization of sub-grid scale clouds

Studies, undertaken for development of parameterization schemes of condensation that appears on a sub-grid scale, have almost exclusively been concerned with moist convection. There are

consequently very few papers to which specific references can be made. Sasamori (1975) proposed a statistical model that could be applied in numerical models with coarse grids (GCM). Hence, Sasamori's major concern is to find representative mean values for cloudiness, liquid water content and rate of precipitation. In a recent paper, Sommeria and Deardorff (1977) discussed the problem of describing a fractional cloud coverage in a grid box. However, they pay specific attention to non-precipitating cumulus clouds. In the sequel, we will make some general observations on this topic. A specific application will then be demonstrated in Subsection 3.2

Let us first remind ourselves that the type of condensation that we are concerned with may be of sub-grid scale not only in the horizontal, but also (perhaps even more likely) in the vertical. Some of the general comments to follow are applicable in both respects, while some will be specific for the lateral extention.

The obvious implication of accounting for sub-grid scale condensation is that it appears before the large-scale relative humidity, U , has reached 100 %. Thus, we have to assess a threshold value U_0 , at which condensation may start, provided that the basic condition of large-scale convergence of water vapour is fulfilled. This threshold value is of course a function of several factors, of which we will qualitatively examine those that appear to be most influential.

The shape of the earth's surface seems to be an important factor in this context. We may infer that generally the value of U_0 should be smaller over hilly and mountineous terrain than over flat areas, like for example the sea surface. The influence of the underlying ground is probably pronounced only in the first 1-2 km above the surface. Strength and direction of wind has also to be considered in this connection. For example, consider a mountain ridge that is contained in a grid square. Then, with the wind direction perpendicular to the ridge, condensation may appear only on the windward side, whilst the air would be relatively dry on the lee side. If the wind is blowing parallel

to the ridge, we may expect that this affects the condensation situation very little. So, in the former case, U_0 should be given a smaller value than in the latter case. In conjunction with this example, we may also raise the question how to determine, whether or not, a grid-square shall be allowed to become filled with clouds.

The above example also indicates that U_0 generally should be a decreasing function of the grid size, because the larger the grid-square is, the more likely it is that merely a fraction of it contains condensation.

The fact that synoptic systems with their associated condensation regions are moving must also be considered, so that such cloud systems can be taken into account, not only while they are filling the whole box, but also during the time they are entering or leaving it. The principle implication of this is obvious, but it is less clear how to formulate practically useful algorithms that have a fair degree of generality.

Regarding sub-grid scales in the vertical, we note that thin cloud layers often are associated with temperature inversions. So the general task in this connection is to express the probability for the existence of a temperature inversion between two grid levels. The further judgement, whether or not a cloud deck should exist has to be based on the (conceived) lapse rate and the humidity situation.

So far we have only regarded the threshold, at which condensation may be assumed to start. In addition to this, relations that describe the further evolution of the relative humidity have to be deduced. Here we find an analogy with the parameterization of the conversion of droplets to drops in the model of the isolated cloud. Namely, we now have to describe how the converged water vapour is shared between a continued feeding of the existing cloud and forming of additional cloud elements. Furthermore, referring to the orographic effects, we may imagine that there are many cases, in which the grid area never becomes completely overcast, suggesting that an upper limit, less than 100 %, of the relative humidity, sometimes has to be employed.

3.2 A specific parameterization scheme

A specific approach to parameterization of non-convective condensation in numerical prediction models (Sundqvist, 1977) will be presented in this section. The derivation of this fairly simplified parameterization scheme, concretely indicates how judgements and decisions have to be made, as to the various levels of parameterization that have been discussed in the preceeding sections. The intention of the approach is to define a scheme that provides the rates of heating and precipitation, as well as the cloud water content. It is assumed that the condensation fills the whole depth between consequative coordinate levels in the vertical, hence, the fractional coverage, which is discussed, applies to the horizontal spread.

We will thus consider the following system of model equations

$$\frac{\partial \theta}{\partial t} = A(\theta) + \frac{\theta}{T}\frac{Q}{c_p} \tag{3.23}$$

$$\frac{\partial q}{\partial t} = A(q) - \frac{Q}{L} \tag{3.24}$$

$$\frac{\partial m}{\partial t} = -\nabla\cdot(Vm) + \frac{Q}{L} - P + \delta f - \frac{\partial}{\partial p}\left[(\omega + a_c)m\right] \tag{3.25}$$

where in accordance with the discussion at the end of 3.1.1 Q/L is the net condensation rate and P is synonymous with S2; the index has been dropped except on the fall velocity term.

The net, or average, heating is composed of the proper heating due to condensation, Q_c, and evaporation, E , of droplets and raindrops which enter the clear portions of the grid area. Thus, denoting the cloud-free fraction of the unit area by $\underline{a}$ we have

$$Q = (1-a)\,Q_c - a\,(E_c + E_r) \tag{3.26}$$

where the indices c and r respectively refer to cloud/cloud droplets and raindrops. It should be pointed out that we now are not considering evaporation of droplets and drops inside the cloud, implying that Q_c describes the net rate where the proper condensation takes place. The derivation of the continuity equation for m therefore starts from

$$(3.27)\quad \frac{\partial m}{\partial t} = -\nabla\cdot(V_r m) + (1-a)\frac{Q_c}{L} - a\frac{E_c}{L} - P - \frac{\partial}{\partial p}\left[(\omega + a\omega_c)m\right]$$

Introducing (3.26) in (3.27), we then obtain (3.25) where

$$(3.28)\quad S7 = a\frac{E_r}{L}$$

Now, deriving an expression corresponding to S1 (eq. 3.21), we have to keep in mind that $q = U\cdot q_s$ not necessarily is the saturation value, so we have to consider the following relation, when we are eliminating the time derivative of θ between equations (3.23) and (3.24)

$$(3.29)\quad \frac{\partial q}{\partial t} = \frac{\partial}{\partial t}(U q_s) = q_s\frac{\partial U}{\partial t} + U\frac{\partial q_s}{\partial t} = q_s\frac{\partial U}{\partial t} + U\frac{\varepsilon L q_s}{RT}\frac{1}{\theta}\frac{\partial \theta}{\partial t}$$

Utilizing this relation, the aforesaid elimination leads to

$$(3.30)\quad \frac{Q}{L} = \left(M - q_s\frac{\partial U}{\partial t}\right)\left(1 + U S_q\right)^{-1}$$

where

$$S_q = \frac{\varepsilon L^2}{R c_p}\frac{q_s}{T^2}$$

$$M = A(q) - U S_q\frac{c_p}{L}\frac{T}{\theta}A(\theta)$$

We now see that US_q is the same as the quantity F discussed in equation (3.21). The second term of M acounts for possible expansion or compression of the air.

With regard to expression (3.30), we realize that, in order to close our system, we have to find a relation for the rate of change of the relative humidity. That is to say, we must describe the evolution of the condensation and the possible spreading of clouds. (Closing by the assumption $\partial U/\partial t = 0$ yields the simplified version mentioned in the last paragraph of 3.1.1.)

Let us therefore consider the tentative rate of change of q, integrated over the clear area, a, assuming that the flux convergence of q is the same over the whole grid area. Hence

$$(3.31) \qquad \overline{\frac{\partial q}{\partial t}} = a\left[A(q) + (E_C + E_R)/L\right]$$

In analogy with (3.26) we furthermore note

$$(3.32) \qquad U = (1-a)U_s + aU_0$$

where $U_S \equiv 1$ is the saturation relative humidity and U_0 is the relative humidity in the cloud-free fraction of the area.

The relation (3.32) means that if we know the rate of change of a, then we also know the rate of change of U. In order to obtain a closure condition, we now make the following assumption. The change of the amount of vapour in a and given by (3.31), is used firstly for keeping the relative humidity in this area at a fixed value, U_0, and the remaining amount is used for forming a cloud with water content m in a fraction of a, i.e., the humidity is raised from q_0 to m in that fraction, which thus is the change of the size of a. Expressed in our variables, those two rates of change are respectively

$$a\frac{\partial}{\partial t}(q_s - q_0) \equiv a(U_s - U_0)\frac{\partial q_s}{\partial t} \quad \text{and} \quad (q_s - q_0 + m)\frac{\partial a}{\partial t}.$$

In the first expression we have now utilized that both U_S and U_0 are constant in time; the parenthesis of the second expression shows the required humidity rise. Since those two effects feed from the amount given by (3.31) we thus obtain

$$(3.33)\quad \left[q_s(U_s-U_0)+m\right]\frac{\partial a}{\partial t}+a(U_s-U_0)\frac{\partial q_s}{\partial t}=-a\left[A(q)+\frac{E_c+E_r}{L}\right]$$

Then, differentiating (3.32) with respect to time and utilizing the relation between saturation mixing ratio and temperature, we obtain

$$(3.34)\quad \frac{\partial U}{\partial t}=\frac{U_s-U}{q_s(U_s-U_0)+m}\left[A(q)+\frac{E_c+E_r}{L}+(U_s-U_0)\delta_q\frac{c_p}{L}\frac{T}{\theta}\frac{\partial\theta}{\partial t}\right]$$

At the very moment of onset of condensation, $U = U_0$ and the quantities related to condensation are zero and we find by inserting (3.34) in (3.30) that $Q = 0$. However, the convergence of water vapour will increase the relative humidity and at the next moment Q will be non-zero, hence yielding cloud mass (3.25) and at the next moment again, all mechanisms will be at work.

It is worthwhile noting that, provided that a cloud water content exists, the above system should be applied even when the quantity M is negative, which results in a negative Q. It is not until the cloud is completely dissolved, that we can merely work with equations (3.23) and (3.24) with $Q = 0$. It is also interesting to observe that the time of dissolving is definitely shorter than the time of building up, because in the former case the subsiding effects and the precipitation cooperate, while in the latter case they counteract each other.

No specific formulation of the evaporation of cloud droplets, E_c, has been deduced in this paper. This evaporation arises when the droplets leave the outer regions of a cloud and come into the cloud-free portions. The rate, at which the droplets leave their clouds, is very much dependent on the distribution of those in the grid area. For a given percentage coverage,

a continuous cloud deck must yield a smaller rate, than if the cloud is spread in smaller portions all over the grid square. Those factors, connected with some kind of diffusion process, could conceivably describe E_C .

In describing the evaporation from raindrops, it is assumed that this is proportional to the rate of precipitation at the particular level that we are considering and to the subsaturation, $(U_S - U_0)$, since this process takes place in the cloud-free regions. Drops formed at the level in question are not subject to this evaporation, but only those that enter from levels above.

We thus get

$$(3.35) \quad \frac{E_r(p)}{L} = k_r \frac{g}{\Delta p} (U_s - U_0) \tilde{P}(p - \frac{\Delta p}{2})$$

where $\tilde{P}(p-\Delta p/2)$ is the from above integrated precipitation rate at the level $(p-\Delta p/2)$ with possible evaporation in the layers above considered. (In layers with no clouds, the subsaturation is of course $(U_S - U)$.) We may compare expression (3.35) with (3.16) in section 3.1.1, where the evaporation rate is proportional to a power of the precipitation content. We notice that S7 is strongly height-dependent because of the air density and the mixing ratio. We may account for these features in the parameter k_r in (3.35). If we assume a rate of precipitation of 2 mm/h, a subsaturation of 20 % and $k_r = 1$, we obtain 10^{-7} kg/kg s^{-1} from (3.35). If we assume a precipitation content of $0.5 \cdot 10^{-3}$ and consider a level around 800 mb, then $S7 = 4 \cdot 10^{-7}$ kg/kg s^{-1}.

Regarding the vertical flux convergence term in (3.25), this is assumed to be zero, implying the assumption that the cloud has a droplet distribution, such that the average fall velocity is balanced by the upwind of the air.

Our remaining concern is now to deduce a relation for the rate of conversion of droplets to raindrops. Referring back to the parameterization S2 in Section 3.1.1, we may reason that, since

the cloud droplets are the feeders to the precipitation content, it is plausible that this is proportional to the cloud water content. We may also estimate m_r, by taking a typical fall velocity of precipitation (about 5 m/s) and considering reasonable rates of precipitation at various levels. Doing so, we find that m_r has values that are quite similar to typical values of m_c. So, we have reasons to expect that we may get a fair description of the conversion with the aid of the only parameter (m) that we have at disposal in this connection. The function adopted in the present approach is as follows

$$(3.36) \quad P = C_m m = C_0 m \left\{ 1 - \exp\left[-(m/m_r)^2 \right] \right\}$$

where C_0 and m_r are parameters that will be discussed below.

The reciprocal of C_m (and C_0), having the dimension of time, should now reflect a typical time of conversion of droplets to raindrops. We notice that this conversion is very slow as long as m is smaller than m_r, implying that clouds with a low water content will essentially be non-precipitating. As the value of m approaches and then passes the value of m_r, the conversion time shortens considerably and the cloud turns into a well-developed precipitating stage. We thus find that the parameter m_r should be a representative value of the water content, at which a cloud typically starts to rain. The numerical value used in the reference experiment is $m_r = 0.5 \cdot 10^{-3}$, corresponding to 0.5 gm^{-3} at an altitude of 800-850 mb.

Returning to the conversion time, or turnover time as mentioned in Section 2.4, we may now look at some numerical values using the above mentioned value of m_r. With $C_0 = 10^{-4}$ s^{-1}, the shortest conversion time during an evolution will be 2.8 hours. Additional examples of C_m as a function of m are given in Table 3.

Table 3. The conversion time, C_m^{-1}, in hours for a few m-values; $m_r = 0.5 \cdot 10^{-3}$; $C_o = 10^{-4}\ s^{-1}$

	a	b	c	d
$m \times 10^3$	0.15	0.35	0.50	0.65
C_m^{-1}	32	7.2	4.4	3.4

The m-value of column a) in Table 3, is representative of a relatively dense fog, while the columns b), c) and d) show the conversion times for m-values roughly corresponding to those that emerged in the discussion in Section 2.2.

We may also notice that, although no threshold value is employed as in the auto-conversion mechanism (3.10), a similar feature follows from the functional form of C_m.

Regarding plausible altitude../temperature influences on the parameters C_o and m_r, we may refer to the discussions in Section 3.1.1.

The present model has been tested numerically in a one-dimensional version with a prescirbed large-scale conversion of water vapour. The model has ten levels in the vertical, from 100 mb to 1000 mb. The parameters have the following values: $U_0 = 0.85$, $c_o = 10^{-4}\ s^{-1}$, $m_r = 0.5 \cdot 10^{-3}$. At initial time $U = U_0$ and $m = 0$ at all levels.

Figure 13 shows the prescribed vertical velocity and the resulting water vapour convergence, in terms of the maximum possible heating in degrees per day.

Figure 14 exhibits the vertical distribution of cloud water content at 6, 12 and 48 hours. We observe that the high concentrations occur in the lowest part of the cloud. By and large, this seems reasonable with respect to the forcing (Figure 13). However, it is difficult to judge if this is exactly what we should expect. We may recall that the model assumes that the fall velocity and the upwind balance each other, if the droplets were instead

assumed to share the air motion, the distribution would probably be smoothed out somewhat.

The vertically integrated evolution of the condensation is shown in terms of precipitation rate in Figure 15. Curve A is the resulting rate if we assume that all water precipitates immediately and curve C is the predicted rate. Curve B is the ratio C/A. We notice that the building up is fairly slow at the beginning and that a relatively fast transition to a pronounced rainfall rate takes place between 5 and 10 hours.

In Figure 16 is shown an experiment with two layers of condensation. To inhibit condensation at certain levels, the relative humidity was set well below the threshold value, as given by the column $t = 0$ in the figure. The resulting cloud water content at 48 hours is shown and the relative humidity at that time is given in the right hand column of the figure. We see that a fairly feable precipitation from the upper layer has raised the relative humidity somewhat in the clear middle layer, while a more pronounced rise is observed in the layer nearest to the ground as a result of the intenser rainfall there.

A few more experiments have also been carried out in order to investigate the sensitivity to parameters and to external forcing, the results of which may be found in the referenced paper (Sundqvist, 1977).

4 REVIEW OF VARIOUS APPROACHES TO INCLUDING CONDENSATION IN NUMERICAL PREDICTION MODELS

General reference: GARP Doc. (1974)

As remarked earlier in this text, there has been very little done on elaborate modelling of non-convective condensation. Approaches presently adopted in numerical weather prediction models and GMCs are therefore quite similar, so we will essentially look at

such features that appear to be particular to one model or one research group. (Models mentioned by name without particular reference may be found in the above general reference.)

Generally we may divide the various approaches into two major groups, one in which the condensation effects are dynamically interplaying with the model motion, and another one, where various aspects of condensation are diagnostically calculated by utilizing variables provided by a numerical model. The way of obtaining the amounts of released latent heat and precipitation is principally the same in all approaches and it suffices to refer to the discussions connected to equations (3.21) and (3.30) of the present description.

Regarding the first mentioned group of approaches, it is appropriate to begin with a slight modification of the last statement of preceeding paragraph. Namely, in some models, the heating and the associated precipitation are obtained by the assumption that saturation is at hand provided that the upward vertical velocity is greater than a given value. Hence, those models do not contain an explicit prognostic equation for the humidity. (As an example of this type of approach see Bengtsson, 1967.)

Some models (but surprisingly few) account for evaporation of raindrops when those pass through subsaturated layers (see, e.g., Bushby and Timpson, 1967).

The estimation of cloudiness is not related to the other condensation calculations in any model (to the author's knowledge). In the RAND Global Model, however, it is assumed that the sky is overcast in the regions of condensation. The NCAR GCM connects the cloudiness to the relative humidity by a linear relationship, with the constraints that the vertical velocity must be greater than -2 cm/s and the relative humidity greater than 75 %.

In the GFDL and the NCAR GCMs it is distinguished between snowfall and rainfall. The precipitation is considered to be in the form of snow, if the freezing level is no higher than 350 m in the former model, and the first level, above the

ground (1.5 km) in the latter.

Concerning the other group of approaches, we should mention the elaborate model by Davies and Olsson (1973), which is in operational use at the Canadian Meteorological Center. The model contains many parameters, which are related to the geographical location as well as to the synoptic situation. The tuning of these parameters follows the intention to facilitate forecasting of so-called trace values of precipitation, as well as maximum values. These aspects in conjunction with the fact that the model is applied to short range forecasting, implies that no special attention has been paid to energy consistency, so this model can hardly be used in, for example, water budget calculations. The model does not consider cloudiness, but merely precipitation.

Being well aware of the chance that some relevant examples or references have been missed in the above (due to ignorance), it nevertheless seems appropriate to state, that there is indeed need and room for further research and development regarding treatment of condensation in numerical prediction models. The formulation of parameterization of sub-grid scale cloud cover may be specially emphasized.

5 REFERENCES

Anderson, R K, Ferguson, E W, Oliver, V J, 1966. The use of satellite pictures in weather analysis and forecasting. WMO Technical Note No 75.

Arakawa, A, 1975. Modelling clouds and cloud processes for use in climate models. GARP Publications Series, No 16. (ICSU/WMO) pp 183-197.

Bader, M J, and Roach, W T, 1977. Orographic rainfall in warm sectors of depressions. Quart. J. R. Met. Soc., Vol 103, pp 269-280.

Bengtsson, L, 1967. Dynamical weather prediction Part B. Compendium in dynamic meteorology. Swedish Meteorological and Hydrological Institute (SMHI).

Bergeron, T, 1935. On the physics of cloud and precipitation. Proc. 5th Assembly UGGI Lisbon, Vol 2.

Bergeron, T, 1951. A general survey in the field of cloud physics. Intern. Union Geod. Geophys., Assoc. Meteorol. Brussels, 1951, Ninth Gen. Assembly Mem., pp 120-134.

Bergeron, T, 1965. On the low-level redistribution of atmospheric water caused by orography. Suppl., Proc. Int. Conf. on Cloud Physics, Tokyo, pp 96-100.

Bergeron, T, 1968. Studies of the oreigenic effect on the areal fine structure of rainfall distribution. Met. Inst., Uppsala Univ., Rep. No 6.

Bushby, F H, and Timpson, M S, 1967. A 10-level atmospheric model and frontal rain. Quart. J. R. Met. Soc., London, 93, pp 1-17.

Danard, M B, 1964. On the influence of released latent heat on cyclone development. J. Appl. Met., No 3, pp 27-37.

Davies, D, and Olson, M P, 1973. Precipitation forecasts at the Canadian Meteorological Centre. Tellus, Vol 25, pp 43.57.

Diem, M, 1948. Messungen der Grösse von Wolkenelementen. II. Met. Rdsch. I.

Eliassen, A, 1959. On the formation of fronts in the atmosphere. In "The Atmosphere and the Sea in Motion" (B Bolin, ed.), pp 277-287. Rockefeller Inst. Press, New York.

Eliassen, A, 1962. On the vertical circulation in frontal zones. Geofys. Publikasjoner, Norske Videnskaps-Akad. Oslo 24, pp 147-160.

Fitzgerald, J W, 1974. Effect of aerosol composition on cloud droplet size distribution: A numerical study. J. Atm. Sci. No 5, pp 1358-1367.

Fletcher, N H, 1969. The physics of rain clouds. Cambridge University Press.

Freeman, M H, 1961. Fronts investigated by the Meteorological Research Flight. Meteorol. Mag. 90, pp 189-203.

GARP Doc., 1974. Modelling for the First GARP Global Experiment. GARP Publications Series, No 14 (ICSU/WMO).

GARP JOC Study Conference 1974. The physical basis of climate and climate modelling. GARP Publications Series, No 16, 1975 (ICSU/WMO).

Hindman, E E, Hobbs, P V, and Radke, L F, 1977. Cloud condensation nucleus size distributions and their effect on cloud droplet size distributions. J. Atm. Sci., No 6, pp 951-956.

Kessler, E, 1969. On the distribution and continuity of water substance in atmospheric circulation. Meteorological Monographs, Vol 10, No 32. American Met. Soc., Boston, Mass.

Kuettner, J P, Rider, N E, Sitnikov, I G, 1962. Experiment design proposal for the GARP Atlantic Tropical Experiment. GATE, Report No 1 (WMO).

Lejenäs, H, 1974. Experiences from numerical forecasting with the primitive multi-layer prediction model at MISU. Report DM-12, Dept. of Met., University of Stockholm.

Manabe, S, Smagorinsky, J and Strickler, R F, 1965. Simulated climatology of a general circulation model with a hydrologic cycle. Mon. Wea. Rev., 93, pp 769-798.

Manabe, S, and Wetherald, R T, 1967. Thermal equilibrium of the atmosphere with a given distribution of relative humidity. J. Atm. Sci., No 3, pp 241-259.

Manabe, S, Smagorinsky, J, Holloway, J L Jr and Stone, H M, 1970. Simulated climatology of a general circulation model with a hydrologic cycle: III. Effects of increased horizontal computational resolution. Mon. Wea. Rev., 98, pp 175-212.

Marshall, J S, and Palmer, W McK, 1948. The distribution of raindrops with size. J. of Meteorology, Vol 5, pp 165-166.

Mason, B J, and Jonas P R, 1974. The evolution of droplet spectra and large droplets by condensation in cumulus clouds. Quart. J. Meteor. Soc., 100, pp 23-38.

Mason, B J, 1971. The Physics of Clouds. Oxford University Press.

Mason, B J, 1956. On the melting of hailstones. Quart. J. R. Met. Soc., Vol 82, pp 209-216.

Matveev, L T, 1967. Mainly chapers 19-24 in Physics of the Atmosphere. Israel Program for Scientific Translations, Jerusalem.

Ogura, Y, and Takahashi, T, 1971. Numerical simulation of the life cycle of a thunderstorm cell. Mon. Wea. Rev., Vol 99, pp 895-911.

Palmén, E, and Newton, C W, 1969. Atmospheric Circulation Systems. International Geophysics Series, Volume 13. Academic Press, New York.

Sasamori, T, 1975. A statistical model for stationary atmospheric cloudiness, liquid water content and rate of precipitation. Mon. Wea. Rev., No 12, pp 1037-1049.

Sawyer, J S, 1956. The vertical circulation at meteorological fronts and its relation to fronto-genesis. Proc. Roy. Soc. A 234, pp 246-262.

Sommeria, G, and Deardorff, J W, 1977. Subgridscale condensation in models of nonprecipitating clouds. J. Atm. Sci., No 2, pp 344-355.

Squires, P, 1958. The microstructure and colloidal stability of warm clouds. I. The relation between structure and stability. Tellus, 10.

Storebø, P B, 1976. Small scale topographical influences on precipitation. Tellus, No 1, pp 45-59.

Sundqvist, H, 1977. A parameterization scheme for non-convective condensation including prediction of cloud water content. (To appear).

Twomey, S, 1976. Computations of the absorption of solar radiation by clouds. J. Atm. Sci., No 6, p 1087.

Wegener, A, 1911. Thermodynamik der Atmosphäre. J.A. Barth, Leipzig.

Some relevant texts, not specifically referenced

Arnason, G, and Greenfield, R S, 1972. Micro- and macrostructures of numerically simulated convective clouds. J. Atm. Sci., 89, pp 342-367.

Benwell, G R R, and Timpson, M S, 1968. Further work with the Bushby-Timpson 10-level model. Quart. J. R. Met. Soc., London, 94, pp 12-24.

Browning, K A, and Harrold, T W, 1969. Air motion and precipitation growth in a wave depression. Quart. J. R. Soc., Vol 95, pp 288-309.

Byers, H R, 1965. Elements of cloud physics. The University of Chicago Press.

Dufour, L, and Defay, R, 1963. Thermodynamics of clouds. International Geophysics Series, Vol 6 (ed. J. van Mieghem), Academic Press.

GARP JOC Study Conference, 1972. Parameterization of sub-grid scale processes. GARP Publications Series No 8 (ICSU/WMO).

Jiusto, J E, 1971. Crystal development and glaciation of a super-cooled cloud. Journal de Recherches Atmosphériques, No 2, pp 69-85.

Mason, B J, 197 . Clouds, rain and rainmaking. Cambridge University Press.

Rogers, R R, 1976. A short course in cloud physics. Pergamon Press.

Savijärvi, H, 1972. The relationship between the vertical velocity in a baroclinic model and the occurance of rain and clouds in Finland. Technical Report No 4, Finnish Meteorological Institute.

Trivikrama Rao, S, and Feng, Z-H, 1977. Parameterization of cloud droplets growth by condensation. J. Appl. Met., No 5, pp 532-544.

Ökland, H, 1976. An example of air-mass transformation in the arctic and connected disturbances of the wind field. Report DM-20, Dept. of Met., University of Stockholm.

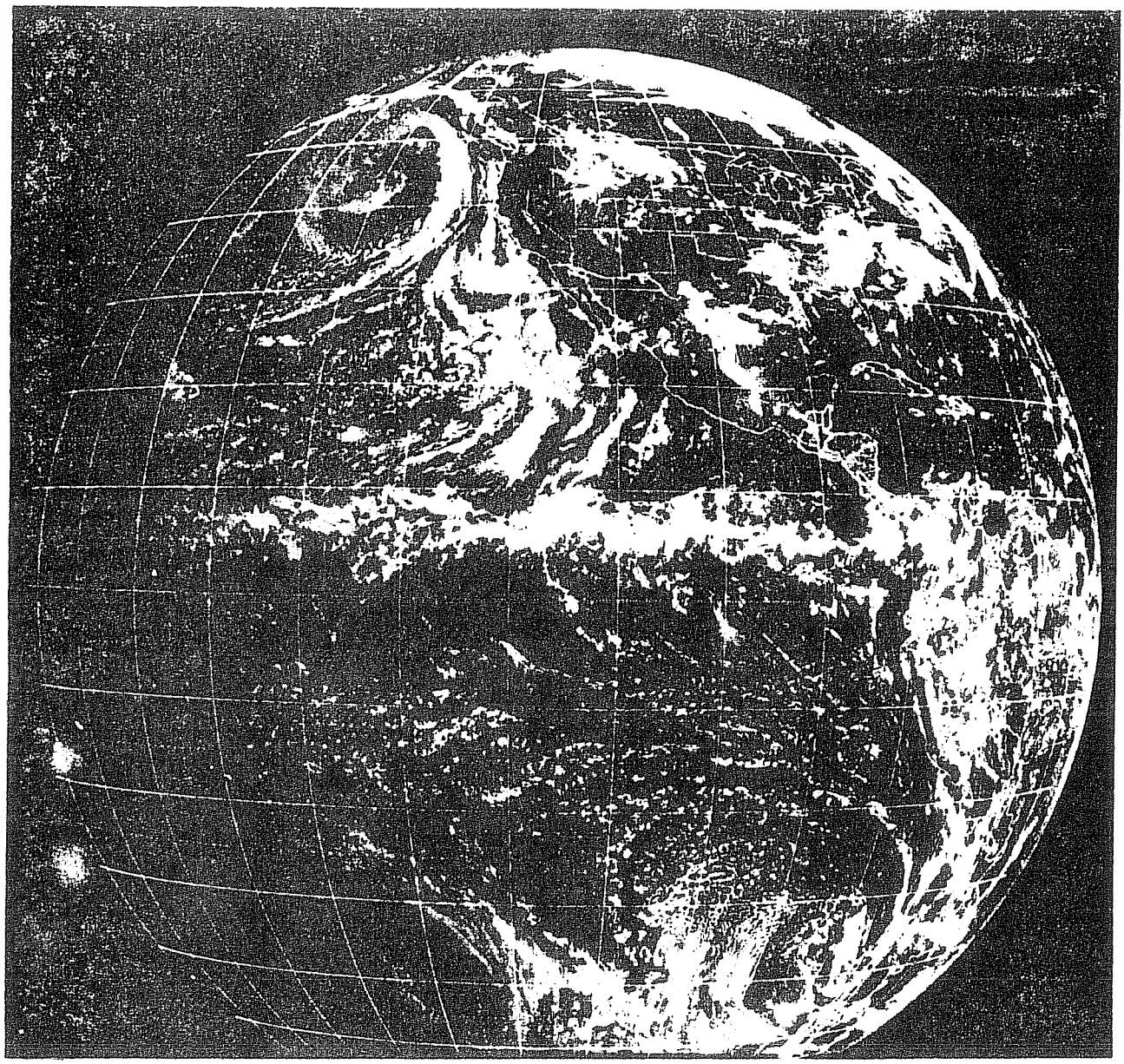

Fig.1 Satellite picture illustrating scales of cloud systems in the amtosphere.

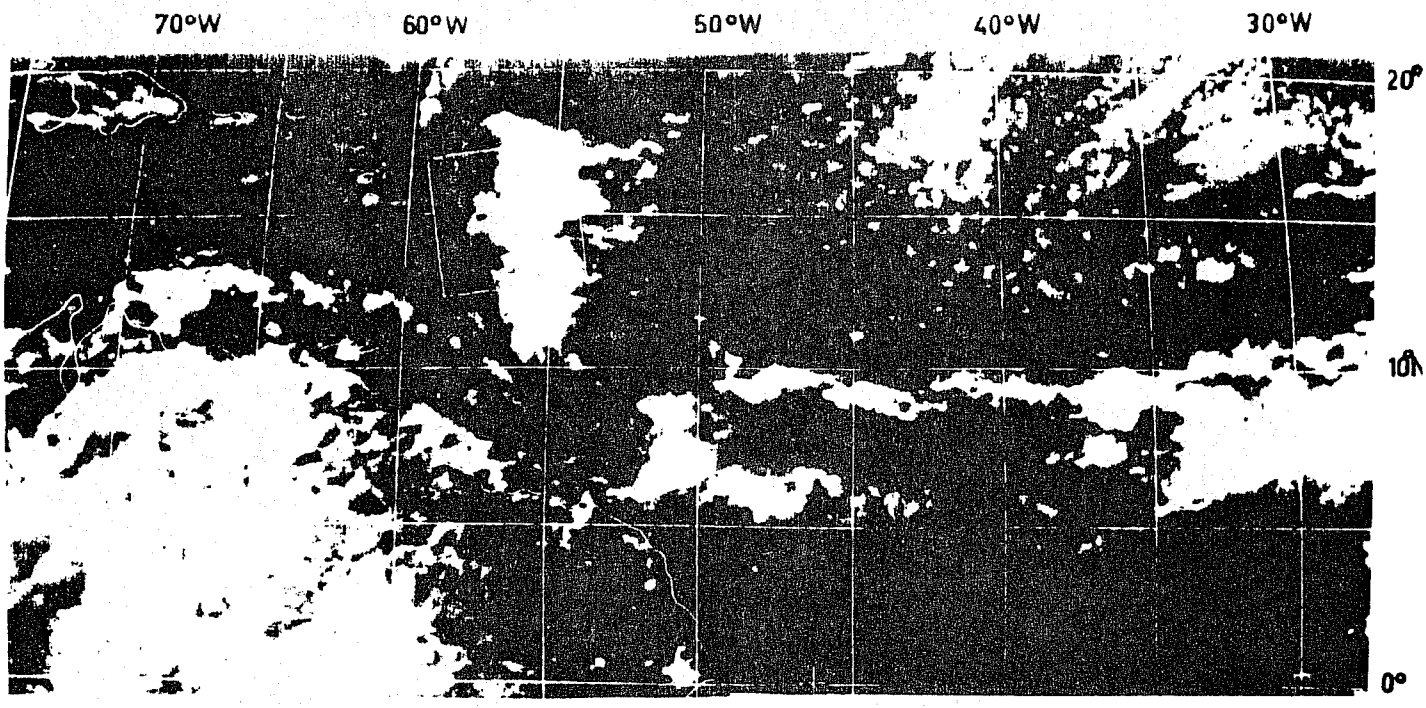

a.

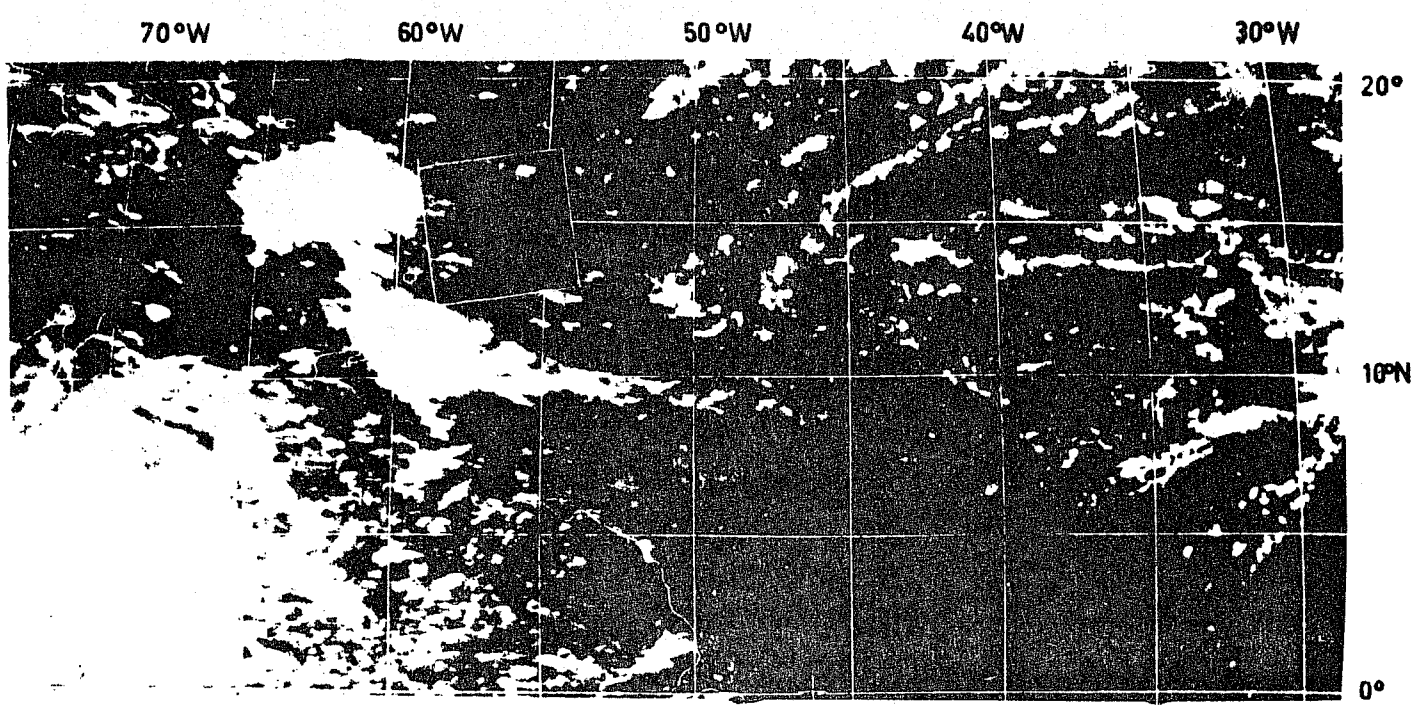

b.

Fig.2 a. ATS-III satellite picture of the central and western Atlantic on 14 July 1969 at 16 GMT, showing a large cloud cluster centred at 15°N 55°W, and a double banded Inter-Tropical Convergence Zone (ITCZ) between 30 and 53°W and between 5 and 10°N.
b. ATS-III satellite picture of the same area 24 hours later. Note double cloud cluster near 60°W and disappearance of the ITCZ. (After Kuettner et. al.,1972)

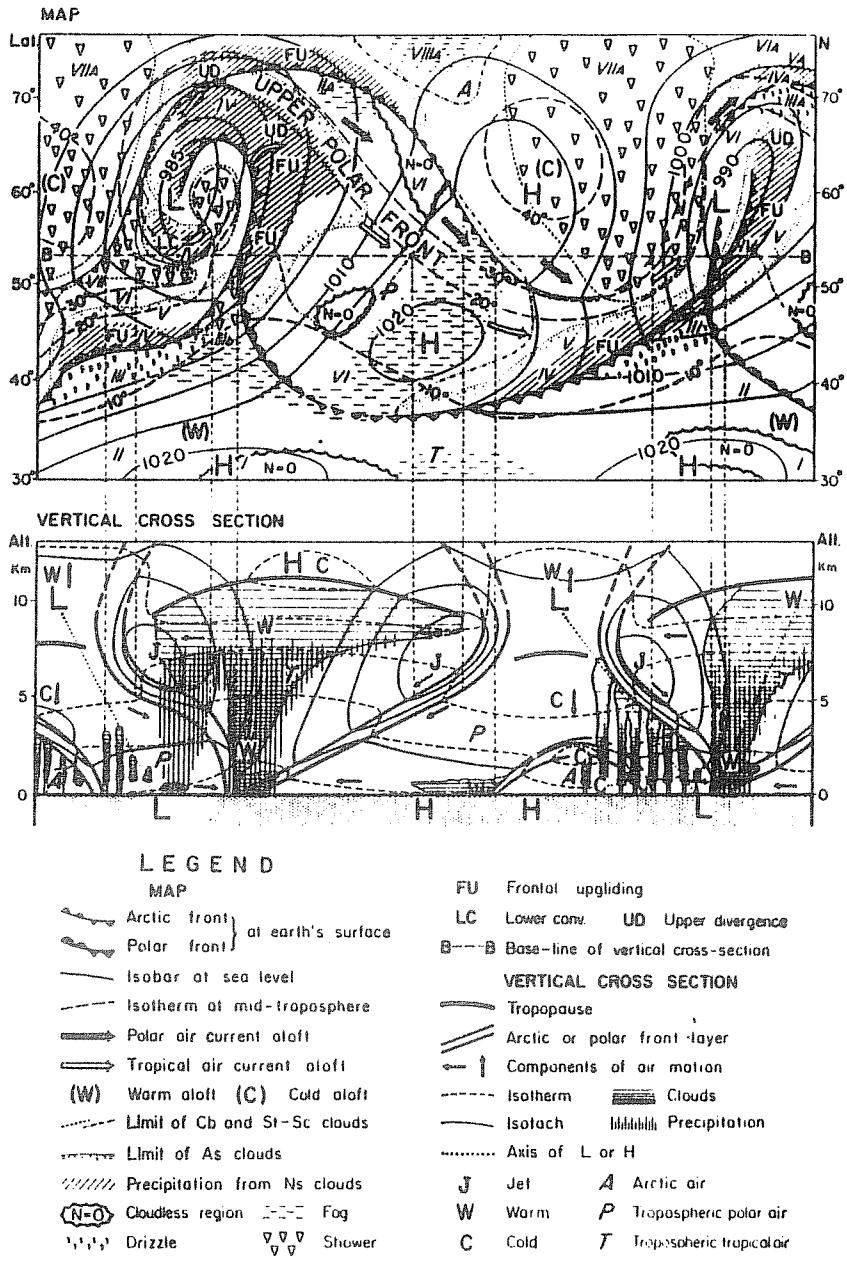

Fig.3 Characteristic distribution of condensation in relation to occluded cyclones over the north Atlantic and western Europe. (After Bergeron, 1951.)

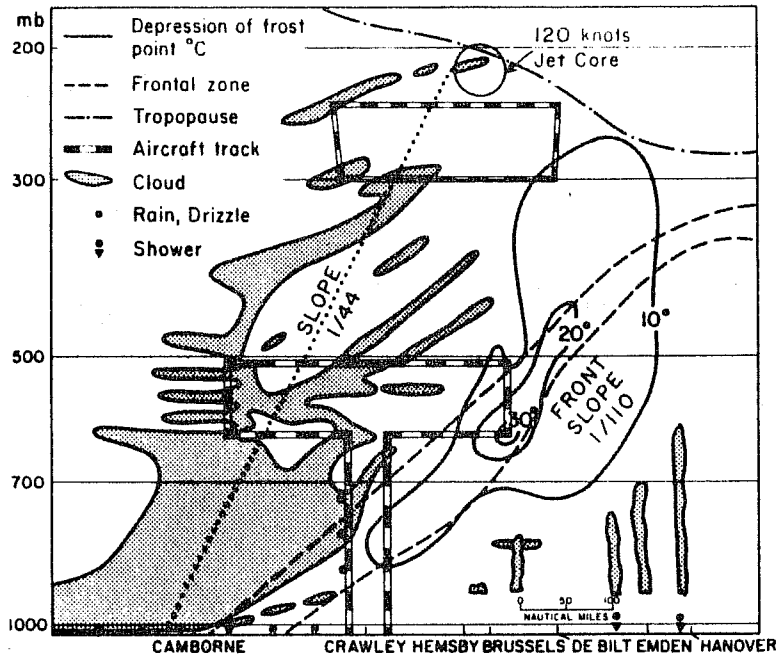

Fig.4. Vertical section along aircraft tracks normal to warm front over southern Britain on Oct.7, 1955, showing clouds and saturation depression relative to frontal layer and jet-stream core. (After Freeman, 1961.)

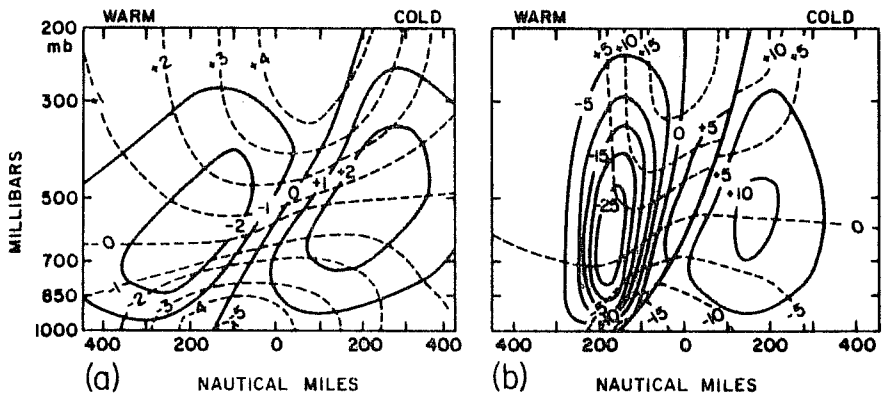

Fig.5 Theoretical distribution of vertical motion (solid lines, mb/hr) and transverse horizontal velocity (dashed lines, kt), resulting from confluence. In (a) the air is dry; in (b) the rising air is assumed to be saturated. In both examples, the magnitude of the basic confluence was assumed to be the same; however, the stabilities and horizontal temperature gradients differed. (After Sawyer, 1956.)

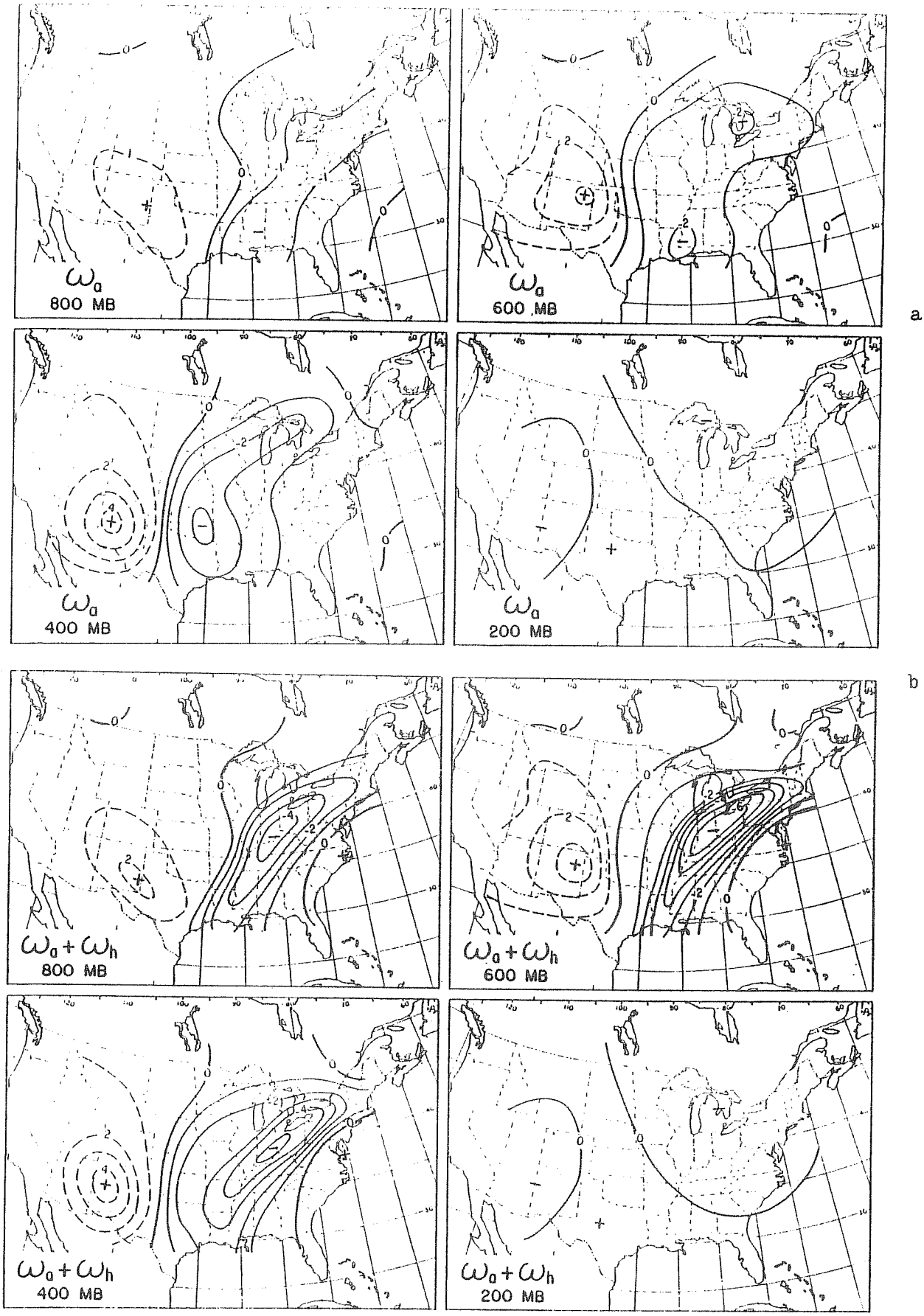

Fig.6 Real data vertical velocity calculated with the aid of the omega-equation. (a) without and (b) with heating by condensation included. (Units: 10^{-3}mb/s). (After Danard, 1964.)

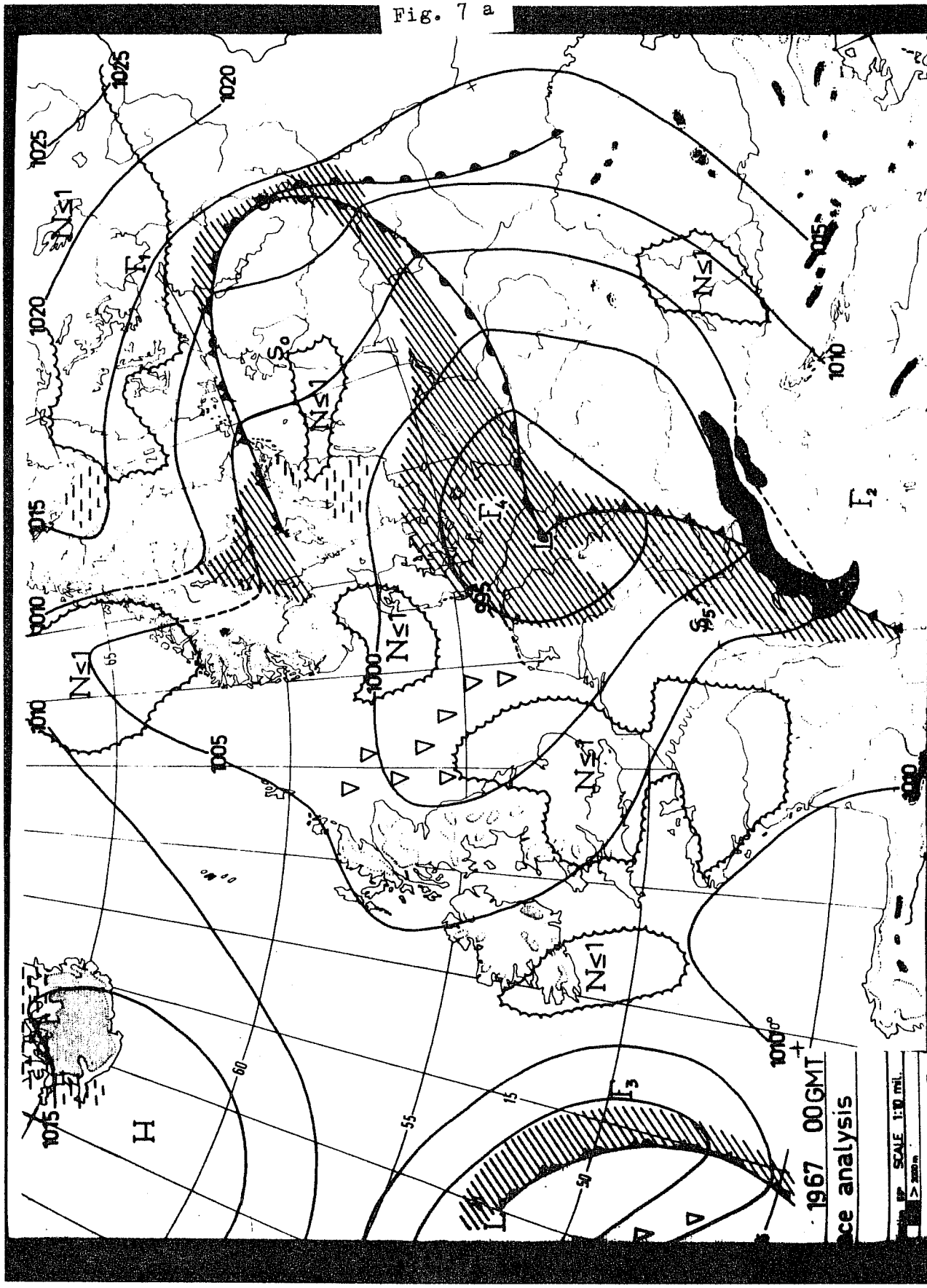

Fig. 7 Illustration of the effect of heating by condensation in the SMHI 3-parameter filtered model. (a): initial surface, (b) verification, (c) 24^h prediction of surface pressure without heating by condensation, (d) same as (c) but with heating. A 150 km grid distance was used. Vertical velocity in cm/s (dashed lines). (After Bengtsson (1967)).

Fig. 7 b

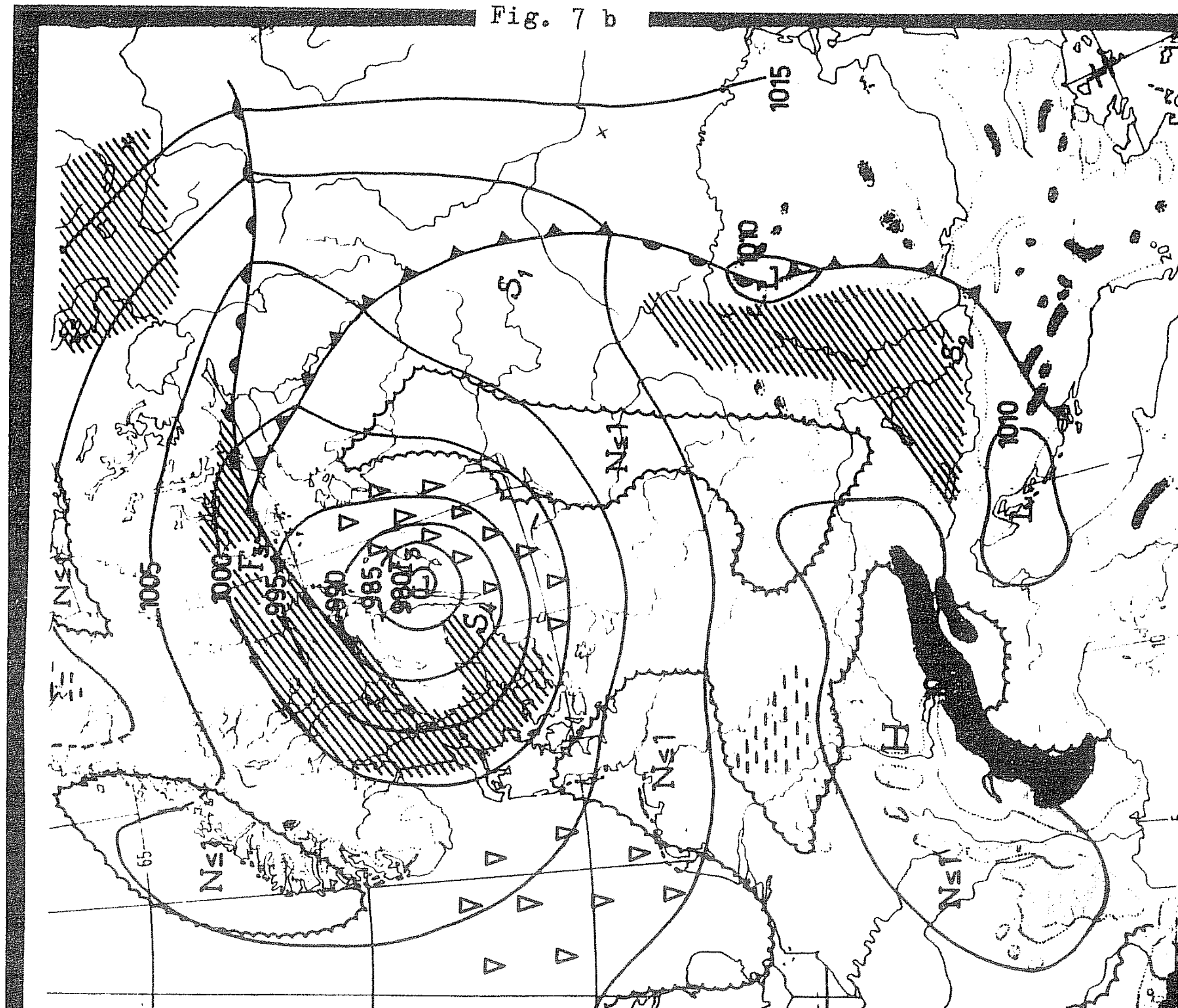

Fig. 7 c

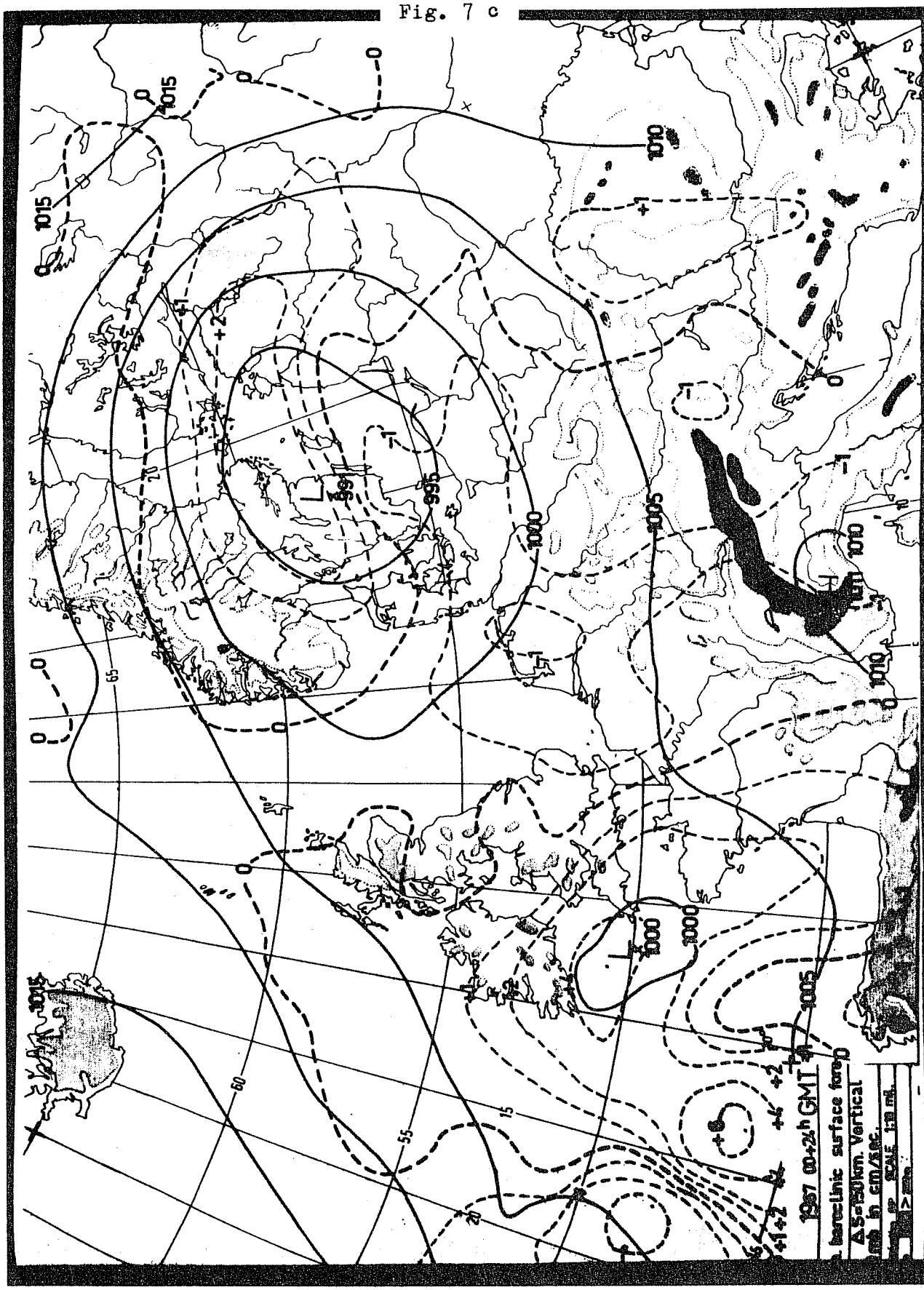
1015
1000
995
1005
1010
1000
1005
1000
1005
baroclinic surface forecast
ΔS=250km. Vertical
mb in cm/sec.
SCALE 1:5 mil.
1957 00+24h GMT

Fig. 7 d

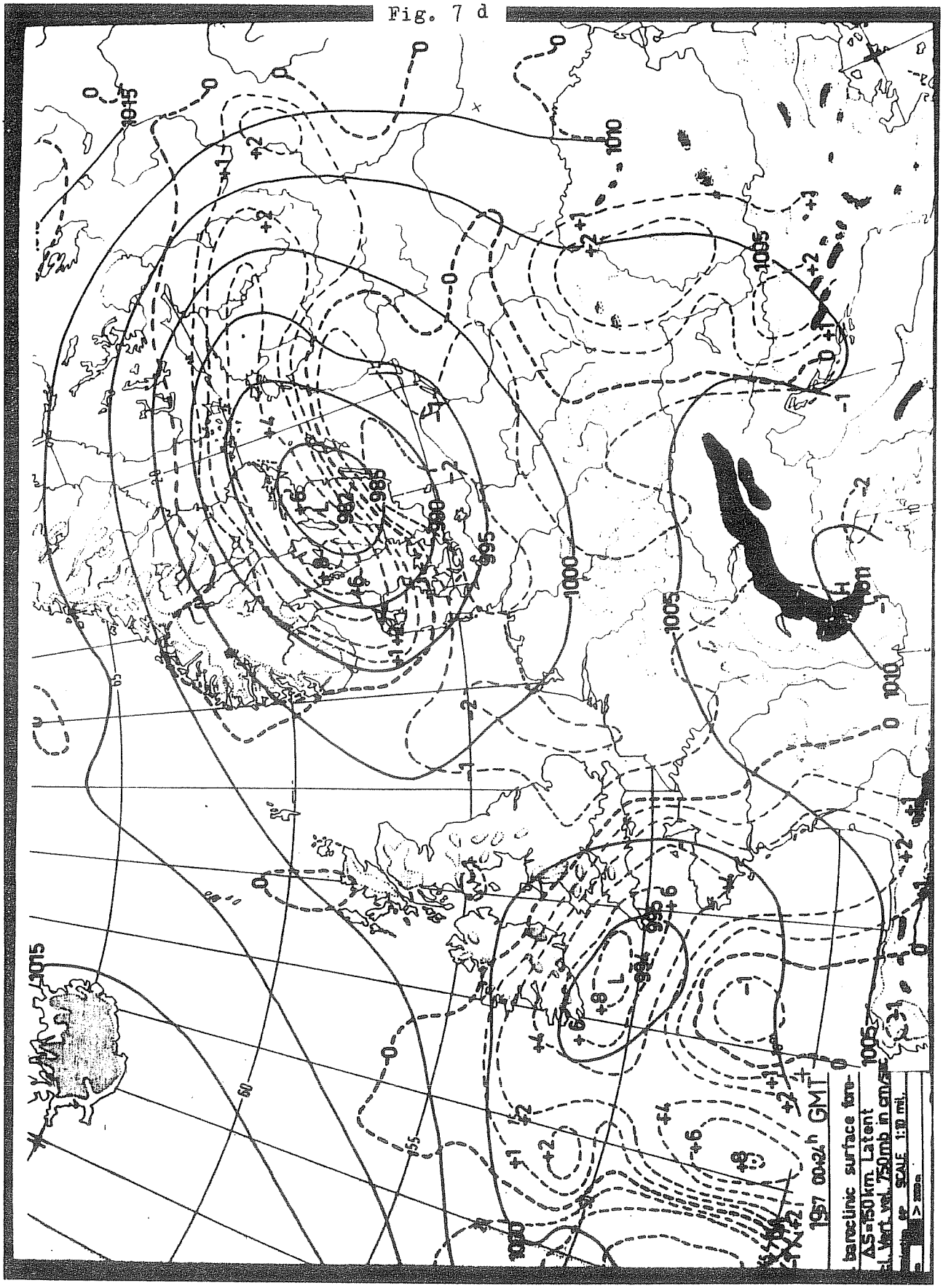
baroclinic surface term
ΔS=150 km Latent
Vert. vel. 750mb in cm/sec
SCALE 1:10 mil.
1967 00h24h GMT

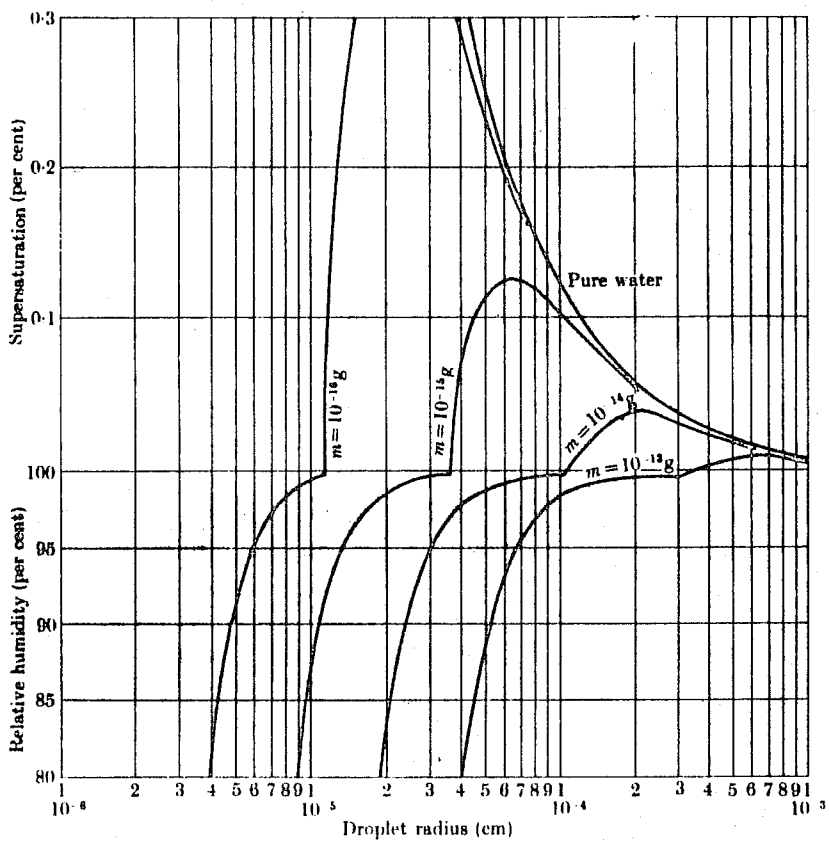

Fig.8 The equilibrium relative humidity (or supersaturation) as a function of droplet radius for solution droplets containing the indicated masses of sodium chloride. (After Mason, 1971).

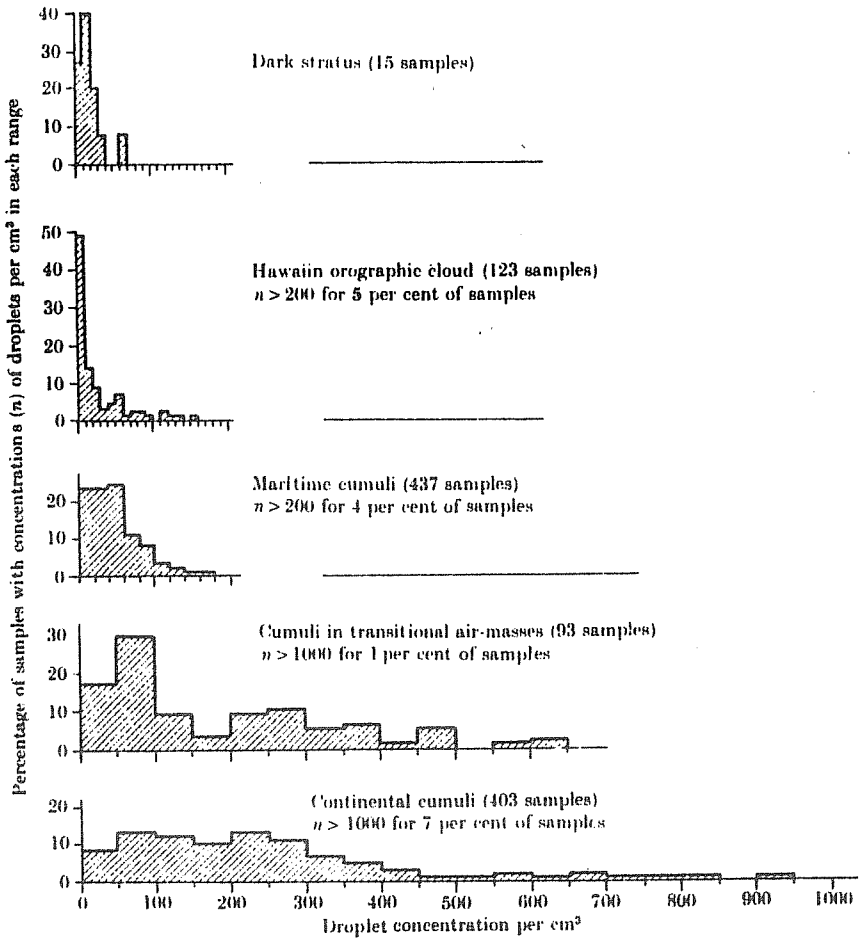

Fig.9a Histograms of the percentages of samples taken in each of five cloud types for which the droplet concentrations fell in the ranges indicated on the horizontal axes. (From Squires (1958a).)

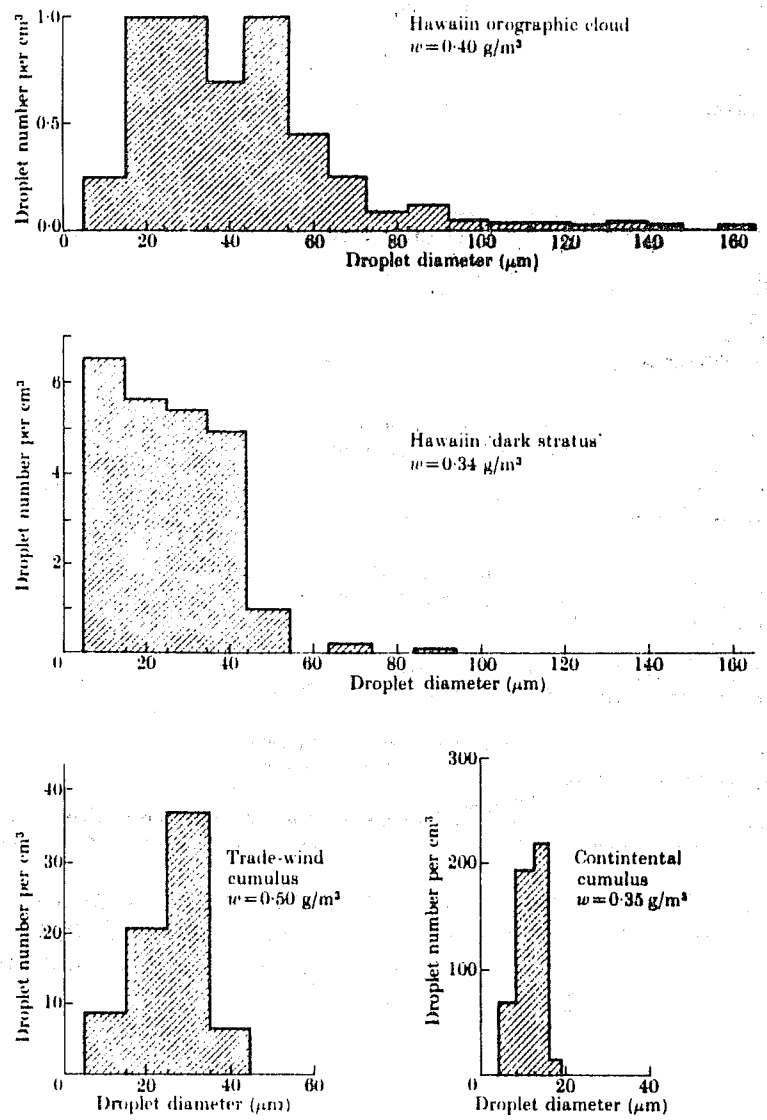

Fig.9b Droplet spectra in clouds of various types, with liquid water contents w as shown. Cumulus samples were taken 2000 ft above cloud base, orographic and dark stratus values are averages. Note change in ordinate scale from figure to figure. (After Squires (1958a).)

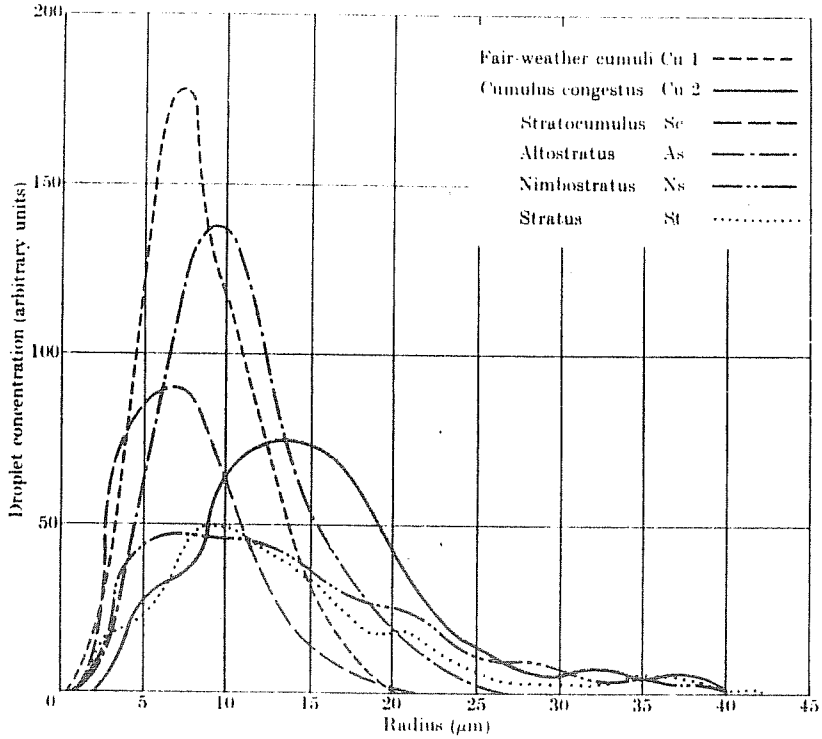

Fig.10a The mean droplet-size distributions of various cloud types. (From Diem (1948).)

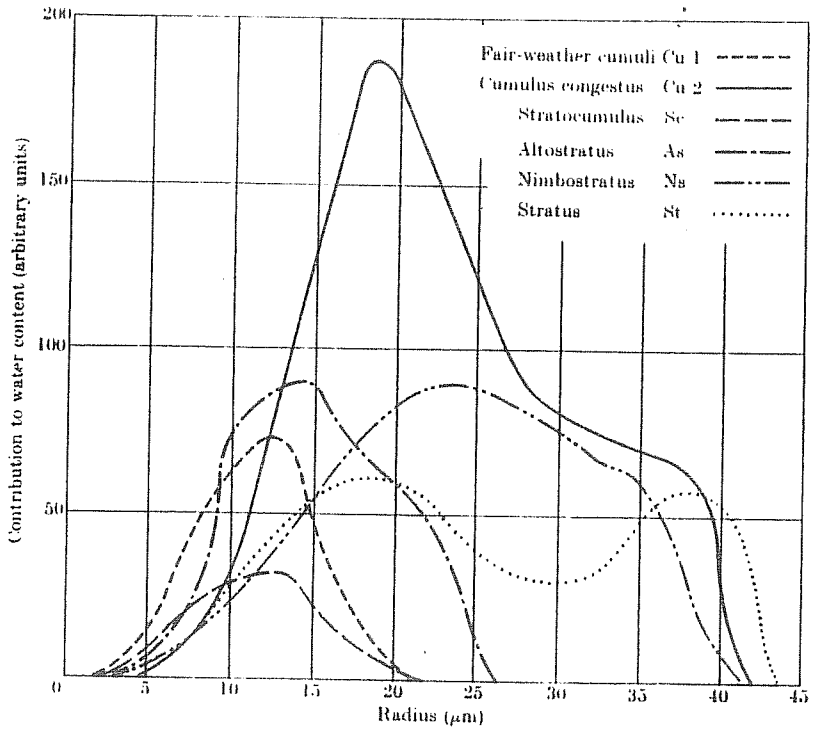

Fig.10b The contribution made by droplets of various sizes to the liquidwater content of different types of cloud. (From Diem(1948).)

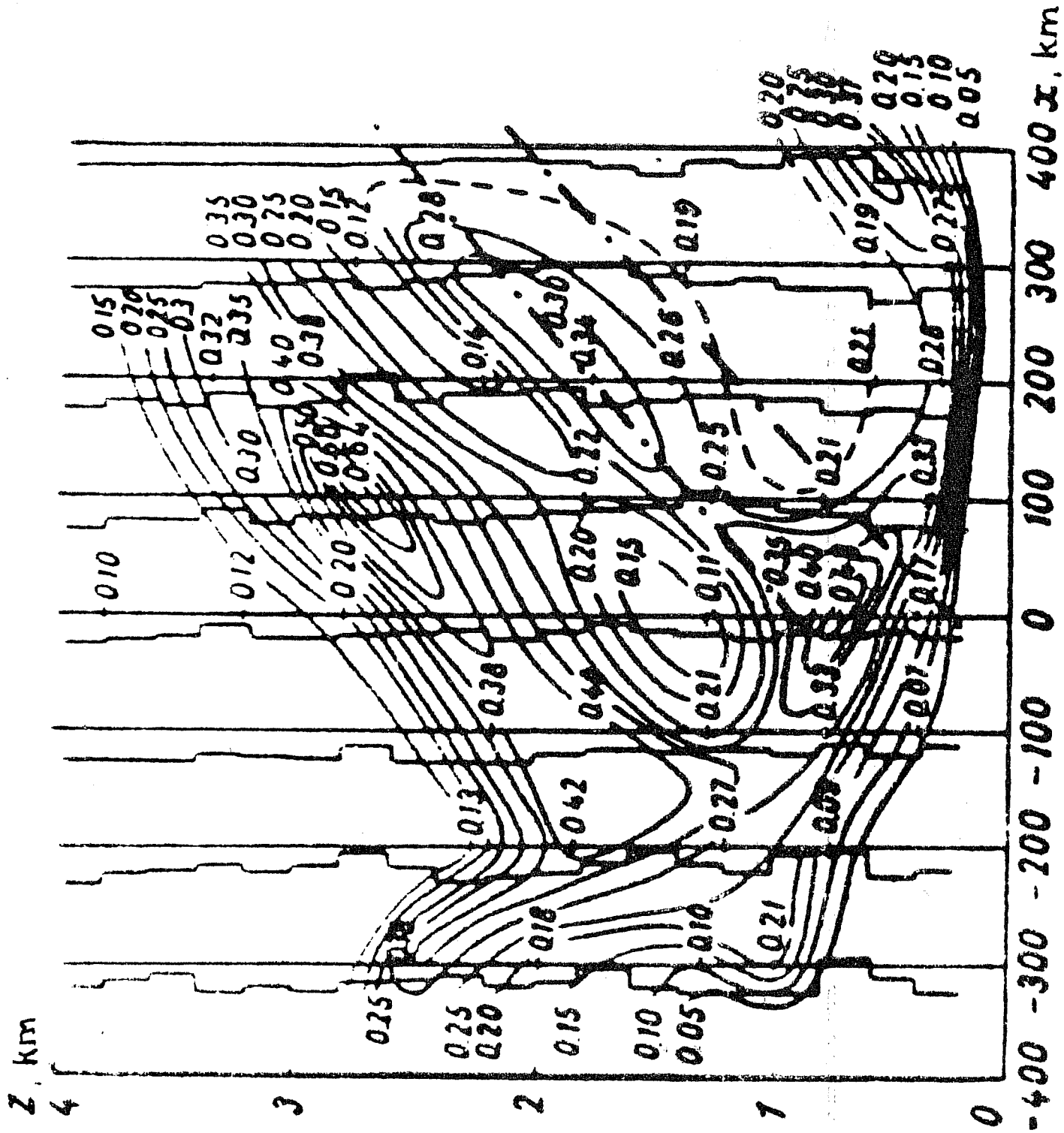

Fig.11 Mean distribution of liquid-water content in the cloud system of a warm front. (After Matveev, 1967.)

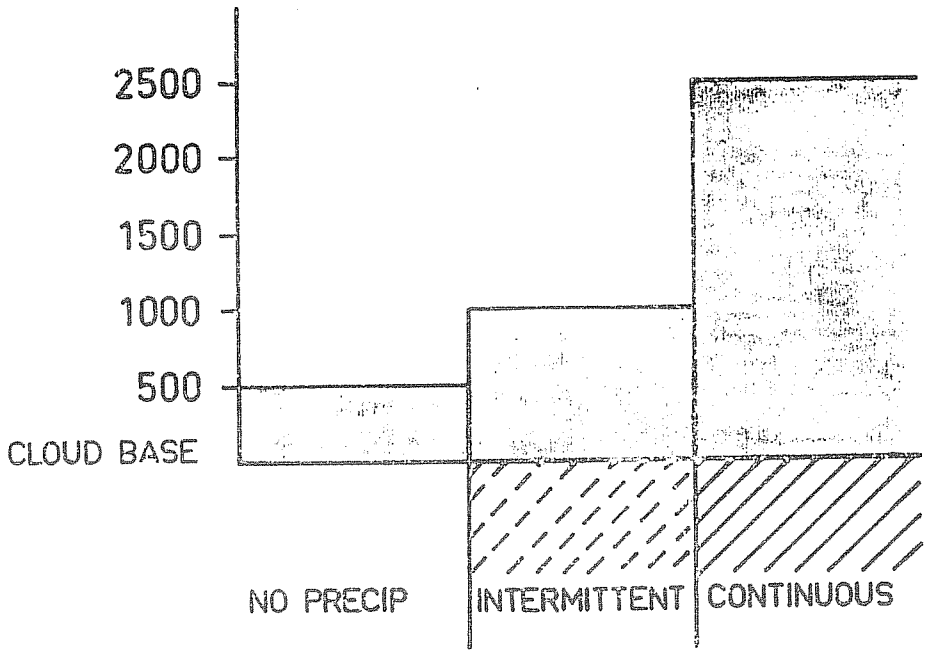

Fig. 12 Illustration of the influence of cloud thickness on rain formation.

Fig. 13 Prescribed vertical velocity in cm/s (————) and prescribed maximum release of latent heat in ^{0}C/day (- - -).

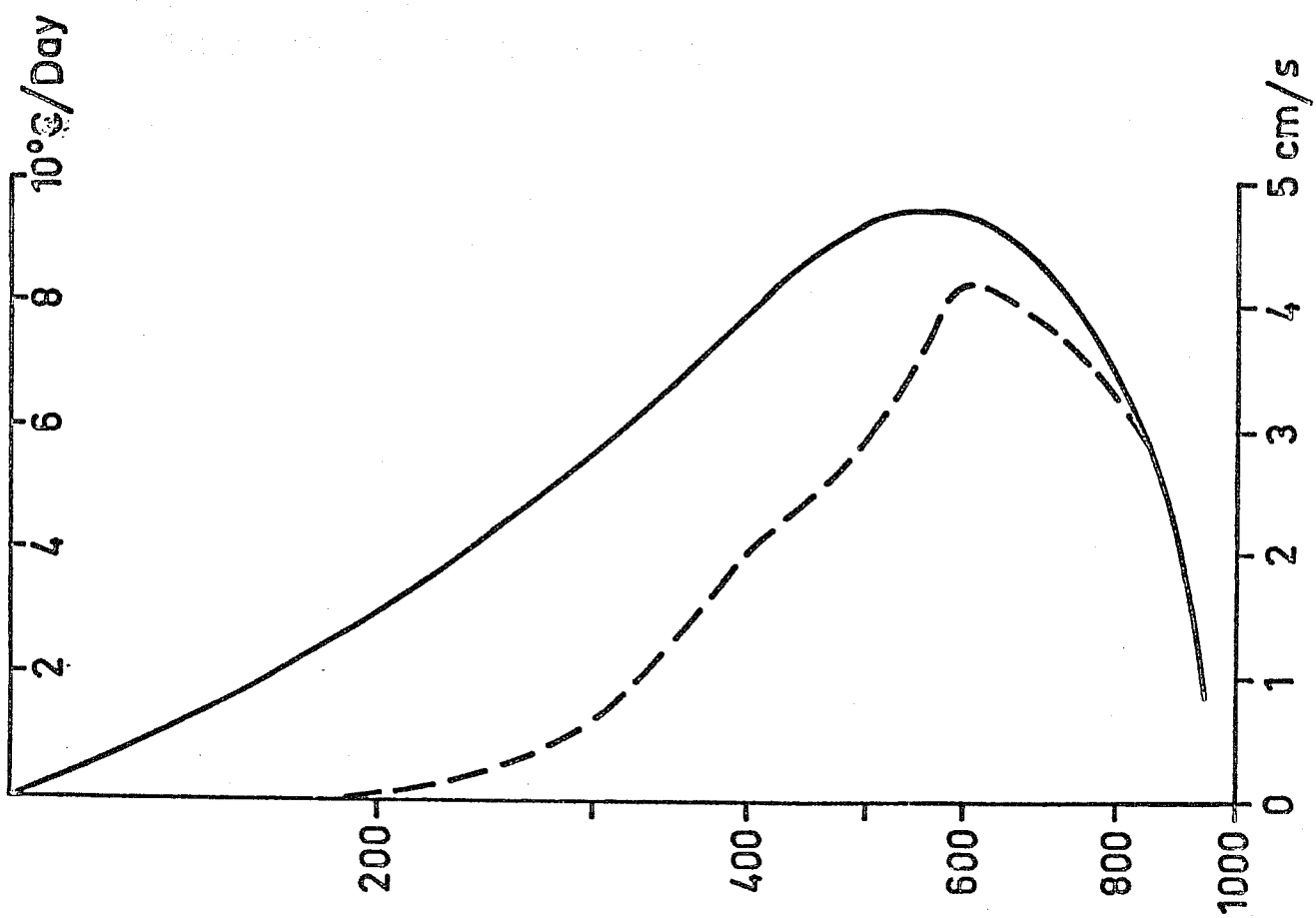

Fig. 14 Reference case: Cloud water (g/m^3) as a function of height at 6 hours (A), 12 hours (B) and 48 hours (C).

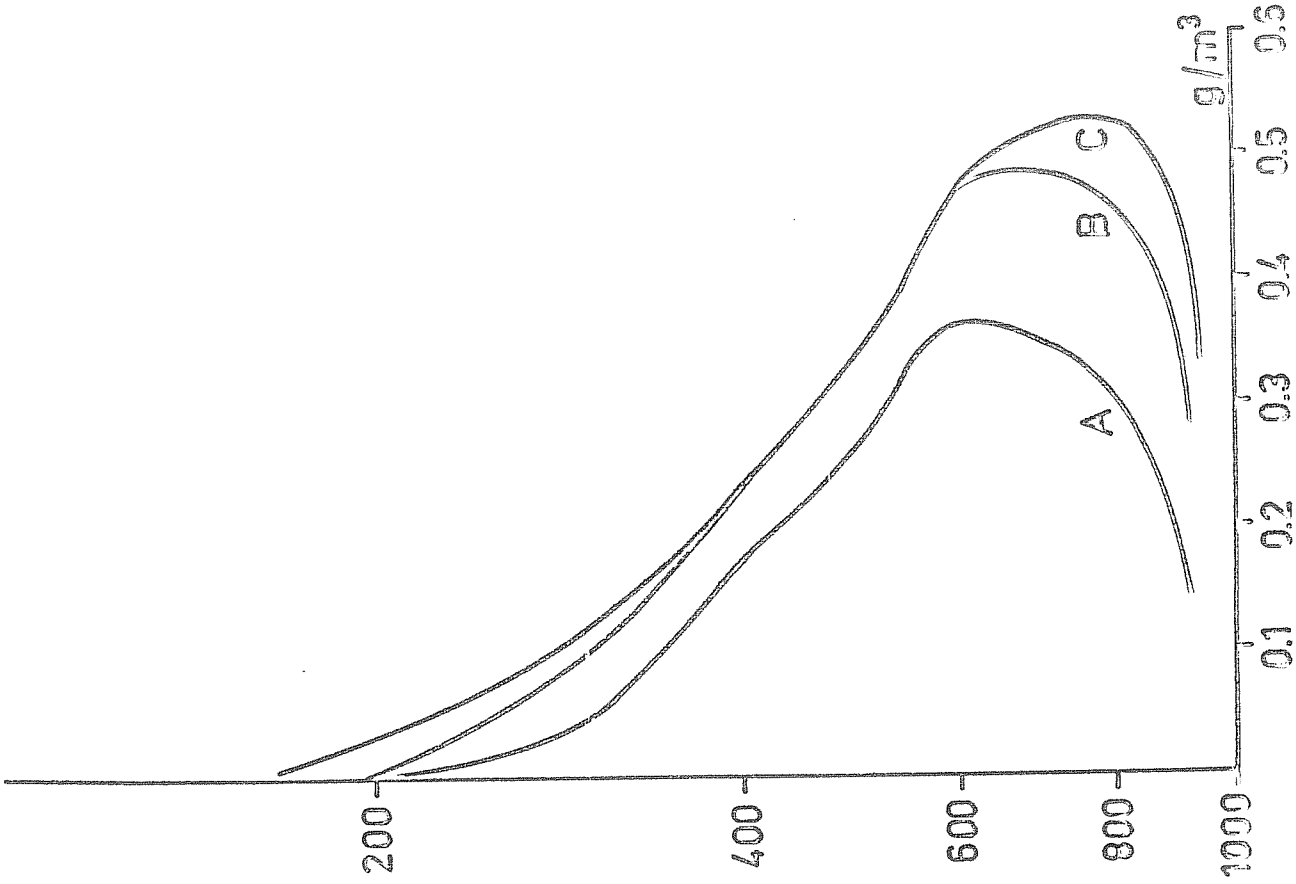

Fig. 15 Reference case: Predicted and diagnostically calculated rates of precipitation (mm/day) and their ratio (%) as functions of time. A = $\tilde{P}_d$, B = $\tilde{P}$, C = $\tilde{P}/\tilde{P}_d$.

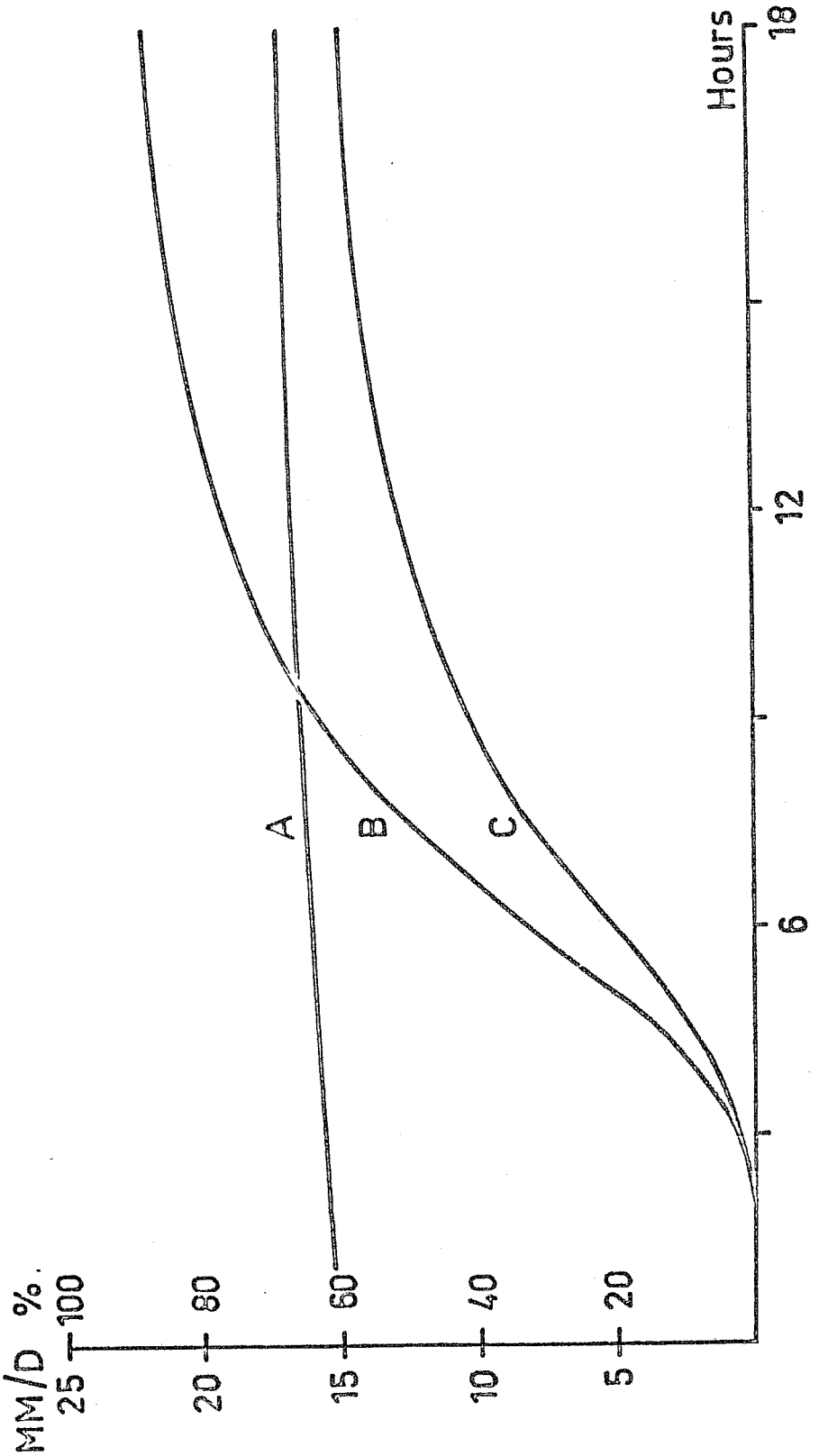

Fig. 16 Case with layers: vertical distribution of cloud water (g/m^3) at 48^h. Columns under U show relative humidity with height at times indicated.